REPORT DOCUMENTATION PAGE

1

Form Approved OMB NO. 0704-0188

The public reporting burden for this collection of information is estimated to average 1 hour per response, including the time for reviewing instructions, searching existing data sources, gathering and maintaining the data needed, and completing and reviewing the collection of information. Send comments regarding this burden estimate or any other aspect of this collection of information, including suggesstions for reducing this burden, to Washington Headquarters Services, Directorate for Information Operations and Reports, 1215 Jefferson Davis Highway, Suite 1204, Arlington VA, 22202-4302. Respondents should be aware that notwithstanding any other provision of law, no person shall be subject to any oenalty for failing to comply with a collection of information if it does not display a currently valid OMB control number.
PLEASE DO NOT RETURN YOUR FORM TO THE ABOVE ADDRESS.

1. REPORT DATE (DD-MM-YYYY)	2. REPORT TYPE	3. DATES COVERED (From - To)
09-09-2014	Ph.D. Dissertation	-

4. TITLE AND SUBTITLE	5a. CONTRACT NUMBER
Maximum Likelihood Fusion Model	W911NF-10-1-0419
	5b. GRANT NUMBER
	5c. PROGRAM ELEMENT NUMBER
	611102

6. AUTHORS	5d. PROJECT NUMBER
Brandon M Jones	
	5e. TASK NUMBER
	5f. WORK UNIT NUMBER

7. PERFORMING ORGANIZATION NAMES AND ADDRESSES	8. PERFORMING ORGANIZATION REPORT NUMBER
Cornell University 373 Pine Tree Road Ithaca, NY 14850 -2820	

9. SPONSORING/MONITORING AGENCY NAME(S) AND ADDRESS (ES)	10. SPONSOR/MONITOR'S ACRONYM(S)
U.S. Army Research Office P.O. Box 12211 Research Triangle Park, NC 27709-2211	ARO
	11. SPONSOR/MONITOR'S REPORT NUMBER(S)
	58094-NS.10

12. DISTRIBUTION AVAILIBILITY STATEMENT

Approved for public release; distribution is unlimited.

13. SUPPLEMENTARY NOTES
The views, opinions and/or findings contained in this report are those of the author(s) and should not contrued as an official Department of the Army position, policy or decision, unless so designated by other documentation.

14. ABSTRACT

In the absence of a global frame of reference, the ability to fuse data collected by multiple mobile agents that operate in separate coordinate systems is critical for enabling autonomy in multi-agent navigation and perception systems. Of particular interest is the ability to fuse rigid body metric environment models in order to construct a global model from the data collected by each agent. This thesis presents a data fusion approach for combining Gaussian metric models of an environment constructed by multiple agents that operate outside of a global reference frame. Common landmarks are combined using a nonlinear least squares approximation, which

15. SUBJECT TERMS
Data association, data fusion, hypothesis testing,maximum likelihood estimation, mobile robot navigation

16. SECURITY CLASSIFICATION OF:			17. LIMITATION OF ABSTRACT	15. NUMBER OF PAGES	19a. NAME OF RESPONSIBLE PERSON
a. REPORT	b. ABSTRACT	c. THIS PAGE			Lang Tong
UU	UU	UU	UU		19b. TELEPHONE NUMBER
					607-255-3900

Standard Form 298 (Rev 8/98)
Prescribed by ANSI Std. Z39.18

Report Title

Maximum Likelihood Fusion Model

ABSTRACT

In the absence of a global frame of reference, the ability to fuse data collected by multiple mobile agents that operate in separate coordinate systems is critical for enabling autonomy in multi-agent navigation and perception systems. Of particular interest is the ability to fuse rigid body metric environment models in
order to construct a global model from the data collected by each agent. This thesis presents a data fusion approach for combining Gaussian metric models of an environment constructed by multiple agents that operate outside of a global reference frame. Common landmarks are combined using a nonlinear least squares approximation, which yields an exact solution under the assumption of isotropic covariance. Rigid body transform parameters and common landmarks are found using a hypergraph registration approach. The approach demonstrates a robustness to outliers in registration by incorporating unit quaternions to reject outliers on a unit sphere. The performance of the approach is evaluated using experimental benchmark datasets collected in natural and semi-structured environments with camera and laser sensors.

MAXIMUM LIKELIHOOD FUSION MODELS

A Dissertation

Presented to the Faculty of the Graduate School

of Cornell University

in Partial Fulfillment of the Requirements for the Degree of

Doctor of Philosophy

by

Brandon Marquese Jones

August 2013

MAXIMUM LIKELIHOOD FUSION MODELS

Brandon Marquese Jones, Ph.D.

Cornell University 2013

In the absence of a global frame of reference, the ability to fuse data collected by multiple mobile agents that operate in separate coordinate systems is critical for enabling autonomy in multi-agent navigation and perception systems. Of particular interest is the ability to fuse rigid body metric environment models in order to construct a global model from the data collected by each agent. This thesis presents a data fusion approach for combining Gaussian metric models of an environment constructed by multiple agents that operate outside of a global reference frame. Common landmarks are combined using a nonlinear least squares approximation, which yields an exact solution under the assumption of isotropic covariance. Rigid body transform parameters and common landmarks are found using a hypergraph registration approach. The approach demonstrates a robustness to outliers in registration by incorporating unit quaternions to reject outliers on a unit sphere. The performance of the approach is evaluated using experimental benchmark datasets collected in natural and semi-structured environments with camera and laser sensors.

BIOGRAPHICAL SKETCH

Brandon Marquese Jones was born in Louisiana in 1983. He grew up in Alexandria and earned a Bachelor of Science degree in Electrical Engineering from Southern University and A&M College. After graduating in 2005, Brandon worked in the aerospace industry for the Boeing Company before joining the MS-PhD program in the School of Electrical and Computer Engineering at Cornell University in 2007 with funding from the NASA Harriett G. Jenkins Predoctoral Fellowship Program (JPFP) and Cornell University Sloan. Brandon spent his time at Cornell working with the Adaptive Communications and Signal Processing Group (ACSP) under the advisement of Professor Lang Tong and the Autonomous Systems Laboratory (ASL) under the advisement of Professor Mark Campbell of the Sibley School of Mechanical and Aerospace Engineering. His work with Prof. Tong and Prof. Campbell stems from an interest in both theoretical and practical problems that relate to the areas of signal processing and robotics. His education was further enriched by research opportunities with the Army Research Laboratory (ARL) of Adelphi, MD., and the Jet Propulsion Laboratory (JPL) of Pasadena, CA., during his time at Cornell.

This thesis is dedicated to my mom and dad for always supporting my goals and educational pursuits.

ACKNOWLEDGEMENTS

This thesis would not have been possible without the continual support of my research committee, family, friends and sponsors. Professor Lang Tong, Professor Mark Campbell and Professor Rick Johnson have cemented themselves among the greatest mentors of my lifetime as it relates to academic research and teaching. Thank you for accepting the role and responsibility of advising me during my time at Cornell. Thank you Mom and Dad for being my support system throughout my time in graduate school. Thank you Uncle Ronnie and Aunt Brenda for being there for me from the very beginning, even before I knew it. Thank you Nanny Cheryl for your many prayers and general support. Thank you to the members of the Adaptive Communications Signal Processing (ACSP) group and the Autonomous Systems Laboratory (ASL) for your friendship and many years of conversation and critical feedback. Thank you Dr. Eddie Tunstel and Professor Ayanna Howard for continuing to provide encouragement and mentorship for so many years after first meeting each of you as an undergraduate intern at JPL. And finally, thank you Ezra Cornell for founding an institution where any person can find instruction in any study.

TABLE OF CONTENTS

LIST OF FIGURES

CHAPTER 1

INTRODUCTION

1.1   Introduction

The general nature of the problem under consideration is to construct a global map of landmarks from the individual efforts of collaborating agents that operate outside of a global frame of reference (examples of such mobile agents are provided in Fig. 1.1). Each agent independently builds a data model of the environment referred to as a *stochastic map* [1, 2]. Constructing a combined global map within a common reference frame from the individual maps of the agents is referred to as a problem of *data fusion in multiple coordinate systems*. Intuitively, the problem has the interpretation of a mathematical jigsaw puzzle: the individual data models are the disoriented pieces and the sought after global map is the completed puzzle.

A benchmark scenario based on the Victoria Park benchmark dataset is illustrated in Fig. 1.2. The satellite image shows the ground truth environment from which the data models are obtained. Trees (landmarks) located in the park are mapped from the global reference frame of the environment to the individual local reference frames of the mobile agents. Each agent thus has an independent, but partial model of the explored environment. The shared objective of the agents is to reconstruct the state of nature from the sensor measurements independently obtained by each agent, which is a common problem encountered in signal processing [3, 4, 5, 6, 7], computer vision and robotics.

Stochastic maps are obtained by independent agents using various estimation techniques. In robotics, the solution to the *simultaneous localization and mapping*
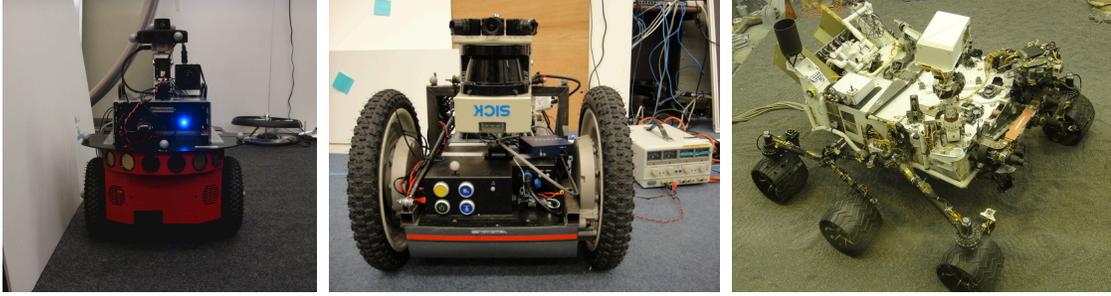
Figure 1.1: Illustration of mobile robotic agents. Land rovers such as (left) Pioneer robots, (center) Segways and (right) the Mars Curiosity rover are examples of mobile agents that operate in environments with limited access to global reference frames. The main topic of this thesis is the data fusion problem of constructing a global metric map from rigid-body data models obtained in the reference frames of each agent.

(SLAM) problem provides an agent with a data model of the environment as a model of landmark locations (see [1, 2, 8, 9, 10] and the references therein). The focus of this thesis, however, is on the fusion – rather than building – of stochastic maps (for completeness, however, an example filtering algorithm used for building metric data models is provided in Appendix A.1). Our starting point is at the individual stochastic maps, which are made available to a fusion agent for the construction of a global map.

The fusion problem with multiple sensor observations is challenging for several reasons, one being that the problem contains both discrete and continuous parts [11, 12]. In order to construct a global map, the fusion agent must first identify common landmarks residing in two separate maps. Using the earlier jigsaw analogy, the solver has to first identify common edges in order to match the individual pieces. Prior to exchanging stochastic maps, the agents are assumed to operate with no prior knowledge concerning the common landmarks (i.e., the common trees when considering the Victoria Park example) that are contained within the individual maps. The problem of matching common landmarks is of a combinatorial nature
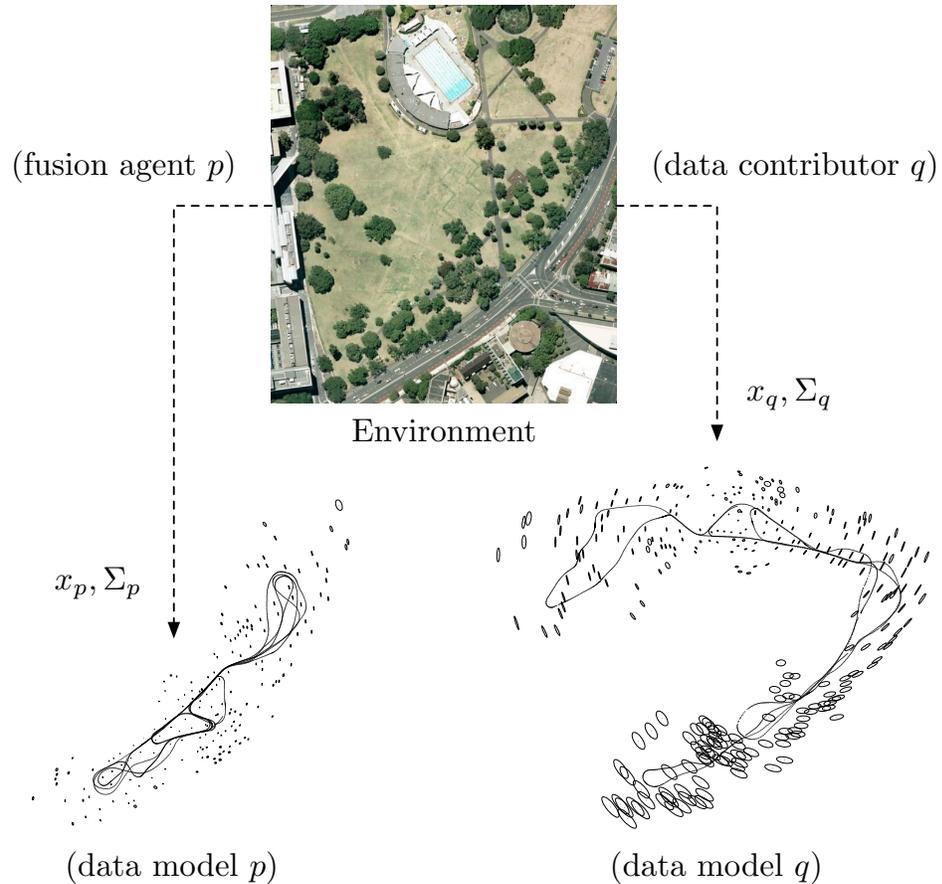
Figure 1.2: A data fusion problem involving rigid-body data models. The data models of agent p (bottom left) and agent q (bottom right) illustrate landmark locations estimated from the sensor observations of two mobile agents operating outside of a global reference frame. Uncertainties in estimation are indicated by ellipses and the path of exploration is shown by dotted lines. Estimation of a common global map from the individual data models, each obtained in a separate coordinate system, requires inferring common landmarks in addition to determining a common frame of reference.

in general, which eliminates exhaustive search as an option for large maps.

Even if common landmarks between two maps have been identified, the agents are faced with the *registration* problem of determining not only the best landmark estimates of common and uncommon landmarks contained by noisy maps obtained in separate coordinate systems, but also to determine the spatial parameters of rotation and translation. Describing this again in terms of the earlier jigsaw analogy:

not only are the pieces disoriented, but the edges are also imprecise (which makes it harder to see how the pieces fit together).

1.1.1 Related work

The data fusion problem considered in this paper has been studied in various forms. Zhou *et al.* [3] derived a two-step iterative optimization procedure for estimating the locations of common targets using range and azimuth measurements obtained by two separate radar sensors. Each sensor observes the locations of targets within a reference frame related by a known displacement. The framework proposed in this paper considers the more general case that the sensor reference frames are related by an unknown displacement and rotation as part of a nonlinear least squares optimization, the solution of which is obtained in closed form. Thrun and Liu [11] proposed an SR-tree (Sphere/Rectangle-tree) search [13] in consideration of the matching problem. Common landmark correspondences and rotation-translation parameters are found using an iterative hill climbing approach to match triplet combinations formed within a small radius of the landmarks in each map. The radius forming the feature vectors of the SR-tree, however, would need to be adaptive in order to generalize to different environments. Estimates of common landmarks are determined separately by a collapsing operation performed on matched landmarks in information form (see Grime and Durrant-Whyte [14], as well as Sukkarieh *et al.* [15], for further reading on fusion using information filtering). Julier and Uhlmann [16] introduced the *covariance intersection* algorithm as an approach to the data fusion problem. Their algorithm uses a convex combination of state information to achieve data fusion, but has the limitation that the input data must be of the same dimension (which is often not the case of

stochastic maps built within different regions of exploration). Tardós *et al.* [17], and later Castellanos *et al.* [18], proposed *map joining* as a technique to enable an individual mobile robot to construct a global stochastic map based on a sequence of local maps. The approach is related to this paper by considering the sequence of local maps as being obtained from separate robots, but requires knowledge of a base reference to construct a global map.

Williams *et al.* [19] considered the fusion problem by providing parameter estimates of the relative rotation and translation between global and local maps. The expressions are derived by observing the geometry of the landmarks within each map. Our approach is distinct from [19] in that the geometry of the landmarks is incorporated in a nonlinear least squares solution based on the maximum likelihood principle. Several authors such as Zhou and Roumeliotis [20], Andersson and Nygards [21], Benedettelli *et al.* [22] and Aragues *et al.* [23] considered rendezvous approaches to the alignment problem. Rendezvous approaches, however, are somewhat restrictive as the agents are required to be in close proximity.

The matching approach of this paper is motivated by the work of Groth [24] and Ogawa [25]. Groth proposed one of the earliest matching algorithms in the context of astronomical point patterns, where a list of star measurements are matched against a known star catalog. In the proposed approach, structured point triplets referred to simply as triangles are used to match the measurements against the catalog. The Groth triangle convention is also incorporated in our approach, however the matching approach of Groth is not practical for large maps since all possible combinations of triangles are considered. An alternative approach was proposed by Ogawa [25], which instead incorporated *Delaunay triangulations* [26] to address the star matching problem. This paper therefore uses Delaunay triangulations

with triangles that follow the Groth convention as a graphical model for matching stochastic maps. Further insight into the structure of the model is found by arranging the triangles in order of increasing perimeter.

1.1.2 Summary of results

A maximum likelihood framework is proposed for the construction of a global map from local stochastic maps. The proposed approach includes 1) a data registration approach referred to as *generalized likelihood data fusion* and 2) a closed form least squares parameter estimation framework for jointly estimating rotation, translation and common landmark parameters. A Gaussian likelihood function is presented as the main proxy for deriving the procedures of each step.

Data registration is a step that is performed in the absence of a global frame of reference, which requires a technique that is affine invariant. To this end, the data models of each agent are modeled as directed hypergraphs constructed from Delaunay triangulations. The hyperedges of each directed hypergraph are constructed from directed Delaunay triangles that follow the Groth convention, which leads to an affine invariant approach for determining common landmarks. The proposed registration approach uses a generalized likelihood ratio as a matching metric in order to obtain globally optimal landmark correspondences from the solution of a linear assignment problem. The GLR metric is computed in closed form and the bipartite matching of hypergraphs is solved in polynomial time as a solution to a linear programming problem.

Once common landmarks are identified, the registration solution of rotation, translation and common landmark locations between the data models is computed

from the vertices of the hypergraph model. The main contributions include 1) a closed-form solution to the parameter estimation problem of determining rigid-body transform parameters as the solution to a nonlinear non-convex optimization, 2) benchmark performance bounds obtained in closed form and a quantitative metric for determining the value of data fusion (which has application to decision making problems that may arise in the area of data fusion) and 3) a robust data registration approach for obtaining for common directed triangles in presence of many outliers.

1.2   Organization

The remainder of this thesis is organized as follows. Chapter 2 introduces the estimation models used to combine data contributed by a fusion agent and a contributing agent, each of which obtain the data is separate coordinate systems. Chapter 3 derives benchmark performance bounds the proposed estimators and includes an analytical study on the value of data fusion. Chapter 4 details a data registration approach based on the generalized likelihood statistics of a hypergraph model constructed from the data of each agent. Concluding remarks are provided in Chapter 6.

CHAPTER 2

MAXIMUM LIKELIHOOD ESTIMATION

2.1   Environment model and available data

A *fusion agent* p is an agent that seeks to build a global metric model of an environment from data exchanged with a contributing agent q. A summary of the parameters used to describe the data fusion problem is as follows.

1. *Common landmarks:* The parameter μ contains the ground truth locations of n landmark locations estimated by both a fusion agent p and a data contributor q.

2. *Uncommon landmarks:* The parameters v_p and v_q contain the ground truth locations of landmark locations estimated by the fusion agent p and the contributor q, respectively, without any overlap on landmark locations.

3. *Rigid-body transformation:* The rotation parameter θ and the translation t define a rigid-body transform between the coordinate systems of the fusion agent and the contributor.

4. *Data:* Landmark locations estimated in the coordinate systems of the fusion agent p and the data contributor q are contained by the data vectors x_p and x_q, respectively. The covariances Σ_p and Σ_q model the uncertainty in the data of agent p and agent q, respectively.

Without loss of generality, the coordinate system of the fusion agent p is defined in the ground truth coordinate system containing the parameters $\{\mu, v_p, v_q\}$.

Some notations used in this chapter are as follows. The symbol $\otimes$ denotes the Kronecker product operator (i.e., $A \otimes B = [a_{ij}B]$) and the matrix I_m is an $m \times m$ identity matrix. The matrix $r(\theta) \in \mathbb{R}^{2 \times 2}$ denotes a rotation matrix

$$r(\theta) \triangleq \begin{pmatrix} \cos\theta & -\sin\theta \\ \sin\theta & \cos\theta \end{pmatrix} \tag{2.1}$$

with rotation parameter $\theta \in [-\pi, \pi]$, with a block diagonal form given by $R(\theta) \triangleq I_m \otimes r(\theta)$. An equivalent form of (2.1) is given by $r(\theta) = I_c \cos\theta + I_s \sin\theta$, where the constant 2×2 matrices I_c and I_s are defined as

$$I_c \triangleq \begin{pmatrix} 1 & 0 \\ 0 & 1 \end{pmatrix} \quad \text{and} \quad I_s \triangleq \begin{pmatrix} 0 & -1 \\ 1 & 0 \end{pmatrix}$$

respectively, with nonzero entries corresponding to the cosine and sine functions of the rotation matrix $r(\theta)$. A *translation input matrix* is a matrix of the form $F \triangleq e_m \otimes I_2$, where e_m is an m-vector with all entries equal to 1.

2.2 Gaussian model of metric maps

Let the random vectors X_p and X_q represent the noisy observations obtained by agents p and q, respectively. Prior to fusion, data is collected in the separate coordinate systems of the agents (i.e., X_p and X_q reside in coordinate systems p and q, respectively). The statistical model of *matched Gaussian maps* is given as

$$X_p = u_p + W_p \tag{2.2}$$

$$X_q = R(\theta)u_q + Ft + W_q \tag{2.3}$$

where $W_p \sim \mathcal{N}(0, \sigma_p^2 I)$ and $W_q \sim \mathcal{N}(0, \sigma_q^2 I)$ are independent zero-mean additive Gaussian noise vectors. The ground truth observed by agent p is then $u_p = (\mu^T, v_p^T)^T$, which is defined in the coordinate system of agent p, and the ground truth of agent q is $u_q = (\mu^T, v_q^T)^T$ in the global reference frame, which is observed in coordinate system q as

$$R(\theta)u_q + Ft = \begin{pmatrix} R_1(\theta) & \\ & R_0(\theta) \end{pmatrix} \begin{pmatrix} \mu \\ v_q \end{pmatrix} + \begin{pmatrix} F_1 \\ F_0 \end{pmatrix} t \tag{2.4}$$

where the subscripts 1 and 0 indicate the partition the map into common and uncommon parts.

In order to separate the data registration and parameter estimation problems, an assumption is made that the common landmarks in both maps are known. The process of obtaining such a matching, however, is nontrivial and combinatorial in general (see Section 4.3 for an affine invariant procedure for determining common landmarks).

2.3 Likelihood decomposition and closed form solution

Estimators of the parameters $\{\mu, v_p, v_q, t, \theta\}$ are derived by considering the likelihood function of the combined global map given by

$$L(\mu, v_p, v_q, t, \theta) \triangleq \eta \exp -\frac{1}{2} J(\mu, v_p, v_q, t, \theta) \tag{2.5}$$

where the function J is defined as

$$J(\mu, v_p, v_q, t, \theta) \triangleq \frac{1}{\sigma_p^2}||x_p - u_p||^2 + \frac{1}{\sigma_q^2}||x_q - R(\theta)u_q - Ft||^2 \tag{2.6}$$

with $x_p = (x_p^{1T}, x_p^{0T})^T$ and $x_q = (x_q^{1T}, x_q^{0T})^T$, corresponding to the structure of u_p and u_q, respectively. By partitioning the problem into common and uncommon parts, it immediately follows that (2.6) decomposes as

$$J(\mu, v_p, v_q, t, \theta) = J_0(v_p, v_q, t, \theta) + J_1(\mu, t, \theta) \tag{2.7}$$

where J_0 is the squared error function of estimating the uncommon landmarks v_p and v_q, including the transform parameters $\{t, \theta\}$, specified as

$$J_0(v_p, v_q, t, \theta) \triangleq \frac{1}{\sigma_p^2}||x_p^0 - v_p||^2 + \frac{1}{\sigma_q^2}||x_q^0 - R_0(\theta)v_q - F_0 t||^2 \tag{2.8}$$

and J_1 is the squared error function of estimating the common landmarks contained by the vector μ, also including $\{t, \theta\}$, specified as

$$J_1(\mu, t, \theta) \triangleq \frac{1}{\sigma_p^2}||x_p^1 - \mu||^2 + \frac{1}{\sigma_q^2}||x_q^1 - R_1(\theta)\mu - F_1 t||^2. \tag{2.9}$$

This decomposition is exploited to minimize the combined error function J by minimizing J_0 and J_1 separately, as stated by the following lemma.

Lemma 1 (Separable optimization) *Let $\{\mu^*, v_p^*, v_q^*, t^*, \theta^*\}$ be the global maximum of the likelihood function L, i.e.,*

$$J(\mu^*, v_p^*, v_q^*, t^*, \theta^*) = \min_{\mu, v_p, v_q, t, \theta} J(\mu, v_p, v_q, t, \theta). \tag{2.10}$$

If the solution $\{\hat{\mu}, \hat{t}, \hat{\theta}\}$ is the global minimum of J_1 given by

$$(\hat{\mu}, \hat{t}, \hat{\theta}) = \underset{\mu, t, \theta}{\mathrm{argmin}}\, J_1(\mu, t, \theta), \tag{2.11}$$

then $\mu^* = \hat{\mu}$, $t^* = \hat{t}$, $\theta^* = \hat{\theta}$ and

$$v_p^* = x_p^0, \quad v_q^* = R_0^T(\hat{\theta})(x_q^0 - F_0 \hat{t}) \tag{2.12}$$

respectively.

Proof: With the decomposition $J = J_0 + J_1$, the proof is immediate by noting that

$$J_0\left(x_p^0, R_0^T(\theta)(x_q^0 - F_0 t), t, \theta\right) = 0 \tag{2.13}$$

for any $\{\mu, t, \theta\}$. $\qquad\qquad\qquad\qquad\qquad\qquad\qquad\qquad\qquad\qquad\Box$

Lemma 1 shows that the maximum likelihood solution of the combined map specified by $u^* = (\mu^{*T}, v_p^{*T}, v_q^{*T})^T$ is obtained from the nonlinear least squares optimization of the non-convex function J_1. A global minimum is obtained by deriving an equivalent expression of J_1 as a sinusoidal form parameterized by the unknown rotation parameter θ, which leads to a closed form solution as stated by the following theorem.

Theorem 1 (Closed form MLE) *The ML estimators of the parameters $\{\mu, t, \theta\}$ are given by the following expressions.*

1. *The MLE of the rotation parameter θ is*

$$\theta^* = \mathrm{sgn}(\beta) \left[\cos^{-1}\left(\frac{\alpha}{\sqrt{\alpha^2 + \beta^2}} \right) - \pi \right] \qquad (2.14)$$

   where $\mathrm{sgn}(\cdot)$ is the signum function. The coefficients α and β are given by

$$\alpha = -x_q^{1T}(I_n \otimes I_c)Qx_p^1 \qquad (2.15)$$

$$\beta = -x_q^{1T}(I_n \otimes I_s)Qx_p^1 \qquad (2.16)$$

   respectively, where $Q = I_{2n} - F_1(F_1^T F_1)^{-1}F_1^T$ with n being the number of common landmarks.

2. *The MLE of the translation t is*

$$t^*(\theta^*) = (F_1^T F_1)^{-1}F_1^T \left[x_q^1 - R(\theta^*)x_p^1 \right] \qquad (2.17)$$

   denoted hereafter as t^*.

3. *The MLE of the common landmarks μ is*

$$\mu^*(\theta^*) = \phi_p^* x_p^1 + \phi_q^* x_q^1 \qquad (2.18)$$

   denoted hereafter as μ^*. The matrix gains ϕ_p^* and ϕ_q^* are given by

$$\phi_p^* = I_{2n} - \frac{\sigma_p^2}{\sigma_p^2 + \sigma_q^2}Q \qquad (2.19)$$

$$\phi_q^* = \frac{\sigma_p^2}{\sigma_p^2 + \sigma_q^2}QR^T(\theta^*) \qquad (2.20)$$

   respectively.

The following lemmas are used in the proof of Theorem 1.

Lemma 2 *The matrix Q is an idempotent and symmetric matrix that commutes with a block diagonal matrix of the form $A = I_n \otimes B$, with $B \in \mathbb{R}^{2\times 2}$.*

Proof: Using the expression for $F^T F$ given by

$$
\begin{aligned}
F^T F &= [e_n \otimes I_2]^T [e_n \otimes I_2] \\
&= [e_n^T e_n] \otimes [I_2^T I_2] \\
&= n I_2
\end{aligned}
$$

it follows that $(F^T F)^{-1} = \frac{1}{n} I_2$ and $F(F^T F)^{-1} F^T = \frac{1}{n} F F^T$ where

$$
\begin{aligned}
F F^T &= [e_n \otimes I_2][e_n \otimes I_2]^T \\
&= [e_n e_n^T] \otimes [I_2 I_2^T] \\
&= \left\{ [e_n e_n^T] \otimes [I_2 I_2^T] \right\}^T \\
&= (F F^T)^T
\end{aligned}
$$

meaning $\frac{1}{n} F F^T = F(F^T F)^{-1} F^T = \bar{Q}$ is symmetric, leading to the conclusion that

$$
\begin{aligned}
Q^T &= (I_{2n} - \bar{Q})^T \\
&= I_{2n}^T - \bar{Q}^T \\
&= I_{2n} - \bar{Q} \\
&= Q
\end{aligned}
$$

which proves that Q is symmetric. Notice that the product of Q with itself is

$$
\begin{aligned}
QQ &= (I_{2n} - \bar{Q})(I_{2n} - \bar{Q}) \\
&= I_{2n} - 2\bar{Q} + \bar{Q}\bar{Q} \\
&= I_{2n} - 2\bar{Q} + \bar{Q} \\
&= I_{2n} - \bar{Q} \\
&= Q
\end{aligned}
$$

which proves that Q is idempotent. The product of the matrix FF^T and the block diagonal matrix $A = I_n \otimes B$ is given by

$$
\begin{aligned}
FF^T A &= [(e_n \otimes I_2)(e_n \otimes I_2)^T][I_n \otimes B] \\
&= [(e_n e_n^T) \otimes I_2][I_n \otimes B] \\
&= [(e_n e_n^T)I_n] \otimes [I_2 B] \\
&= [I_n(e_n e_n^T)] \otimes [BI_2] \\
&= [I_n \otimes B][(e_n e_n^T) \otimes I_2] \\
&= [I_n \otimes B][(e_n \otimes I_2)(e_n \otimes I_2)^T] \\
&= AFF^T.
\end{aligned}
$$

Since $FF^T A = AFF^T$ and $F^T F = nI_2$, it follows that

$$
\begin{aligned}
QA &= [I_{2n} - F(F^T F)^{-1} F^T]A \\
&= A - \tfrac{1}{n}FF^T A \\
&= A - \tfrac{1}{n}AFF^T \\
&= A[I_{2n} - F(F^T F)^{-1} F^T] \\
&= AQ
\end{aligned}
$$

which proves that Q and A commute. $\qquad\square$

Lemma 3 *The sinusoidal form with constant coefficients $\alpha, \beta, \gamma \in \mathbb{R}$ defined as*

$$J_s(\theta) \triangleq \alpha \cos \theta + \beta \sin \theta + \gamma, \ \ \theta \in [-\pi, \pi] \tag{2.21}$$

reaches a global minimum at the value $\theta^* = \Upsilon(\beta, \alpha)$, where the function Υ is defined as

$$\Upsilon(\beta, \alpha) \triangleq \mathrm{sgn}(\beta) \left[\cos^{-1} \left(\frac{\alpha}{\sqrt{\alpha^2 + \beta^2}} \right) - \pi \right] \tag{2.22}$$

where $\mathrm{sgn}(\cdot)$ is the signum function.

Proof: The following proof is elementary in nature and applies for all $\gamma \in \mathbb{R}$ since γ is constant with respect to θ. Consider the trigonometric identity of the form

$$(\kappa \cos \varphi) \cos \theta + (\kappa \sin \varphi) \sin \theta = \kappa \cos (\theta - \varphi) \tag{2.23}$$

with $\kappa \in \mathbb{R}$ and $\theta, \varphi \in [-\pi, \pi]$. By considering the sum

$$\begin{aligned} \alpha^2 + \beta^2 &= (\kappa \cos \varphi)^2 + (\kappa \sin \varphi)^2 \\ &= \kappa^2 \left(\cos^2 \varphi + \sin^2 \varphi \right) \\ &= \kappa^2 \end{aligned}$$

where $\alpha = \kappa \cos \varphi$ and $\beta = \kappa \sin \varphi$, it follows by taking square roots that $\kappa = \sqrt{\alpha^2 + \beta^2}$ so that

$$\alpha \cos \theta + \beta \sin \theta = \sqrt{\alpha^2 + \beta^2} \cos (\theta - \varphi) \tag{2.24}$$

with $\alpha, \beta \in \mathbb{R}$. An expression for the angle φ is found by considering the ratio

$$\frac{\beta}{\alpha} = \frac{\kappa \sin \varphi}{\kappa \cos \varphi}$$
$$= \tan \varphi$$

which leads to the relation

$$\varphi = \tan^{-1}\left(\frac{\beta}{\alpha}\right). \tag{2.25}$$

The arctangent in (2.25) is typically implemented using the atan2 function, which is expressed in closed form as

$$\varphi(\beta, \alpha) = \mathrm{sgn}(\beta) \cos^{-1}\left(\frac{\alpha}{\sqrt{\alpha^2 + \beta^2}}\right) \tag{2.26}$$

as a function of α and β (note that the expression is undefined in the case that $\alpha = \beta = 0$). It directly follows that the sinusoidal form is maximized by the value $\theta_{max} = \varphi(\beta, \alpha)$ and minimized by the value

$$\begin{aligned}\theta^* &= \Upsilon(\beta, \alpha) \\ &= \mathrm{sgn}(\beta)\left[\cos^{-1}\left(\frac{\alpha}{\sqrt{\alpha^2 + \beta^2}}\right) - \pi\right]\end{aligned}$$

by observing that

$$\begin{aligned}\alpha \cos \theta^* + \beta \sin \theta^* &= \kappa \cos\left(\theta^* - \varphi(\beta, \alpha)\right) \\ &= \kappa \cos\left(-\mathrm{sgn}(\beta)\pi\right) \\ &= \kappa \cos\left(\pi\right)\end{aligned}$$

where $\cos\left(\pi\right) = -1$ is the minimum value of $\cos \theta$ on the interval $\theta \in [-\pi, \pi]$. $\quad\square$

Proof: [Proof of Theorem 1] Minimizing (2.38) with respect to (w.r.t.) μ leads to

$$\bar{\mu}(\theta, t) = \frac{\sigma_p^2 \sigma_q^2}{\sigma_p^2 + \sigma_q^2} \left[\frac{1}{\sigma_p^2} x_p + \frac{1}{\sigma_q^2} R^T(\theta)(x_q - Ft) \right] \tag{2.27}$$

and minimizing (2.38) w.r.t. t leads to

$$\bar{t}(\theta, \mu) = (F^T F)^{-1} F^T \left(x_q - R(\theta)\mu \right). \tag{2.28}$$

Using the evaluation $\mu = \bar{\mu}(\theta, t)$ in (2.28) results in the MLE of t as a function of θ given by

$$t^*(\theta) = (F^T F)^{-1} F^T \left(x_q - R(\theta)x_p \right). \tag{2.29}$$

Applying the evaluation $t = t^*(\theta)$ in (2.27) leads to the MLE of μ as a function of θ given by

$$\mu^*(\theta) = \phi_p(\theta)x_p + \phi_q(\theta)x_q. \tag{2.30}$$

Using the symmetry and idempotence properties of the matrix Q (Lemma 2), it follows from the expression (2.30) that

$$
\begin{aligned}
||x_p - \mu^*(\theta)||^2 &= \kappa_p ||x_q - R(\theta)x_p||_{Q^T Q}^2 \\
&= \kappa_p ||x_q - R(\theta)x_p||_Q^2
\end{aligned}
$$

where $\kappa_p = \left(\frac{\sigma_p^2}{\sigma_p^2 + \sigma_q^2} \right)^2$. Similarly, it follows from (2.29) and (2.30) that

$$
\begin{aligned}
||x_q - R(\theta)\mu^*(\theta) - Ft^*(\theta)||^2 &= \kappa_q ||x_q - R(\theta)x_p||_{Q^T Q}^2 \\
&= \kappa_q ||x_q - R(\theta)x_p||_Q^2
\end{aligned}
$$

where $\kappa_q = \left(\frac{\sigma_q^2}{\sigma_p^2 + \sigma_q^2}\right)^2$. Using these simplifications to define

$$
\begin{aligned}
J_1^*(\theta) &\triangleq \frac{1}{2\kappa} J_1(\mu^*(\theta), t^*(\theta), \theta) \\
&= \frac{1}{2}||x_q - R(\theta)x_p||_Q^2
\end{aligned}
\tag{2.31}
$$

where $\kappa = \frac{1}{\sigma_p^2}\kappa_p + \frac{1}{\sigma_q^2}\kappa_q$ and expanding the norm in the right hand side (RHS) of (2.31) as

$$
\begin{aligned}
||x_q - R(\theta)x_p||_Q^2 &= x_p^T R^T(\theta)QR(\theta)x_p + x_q^T Q x_q \\
&\quad -2x_q^T Q R(\theta)x_p,
\end{aligned}
\tag{2.32}
$$

it follows from Lemma 2 that the first term on the RHS of (2.32) reduces to

$$
\begin{aligned}
x_p^T R^T(\theta)QR(\theta)x_p &= x_p^T R^T(\theta)R(\theta)Q x_p \\
&= x_p^T Q x_p
\end{aligned}
\tag{2.33}
$$

so that from (2.31), (2.32) and (2.33), $J_1^*(\theta)$ reduces to

$$
J_1^*(\theta) = \frac{1}{2}(x_p^T Q x_p + x_q^T Q x_q - 2x_q^T R(\theta)Q x_p).
\tag{2.34}
$$

Notice in the last term on the RHS of (2.34) that

$$
\begin{aligned}
x_q^T R(\theta)Q x_p &= x_q^T \left[R_c(\theta) + R_s(\theta)\right] Q x_p \\
&= x_q^T R_c(\theta)Q x_p + x_q^T R_s(\theta)Q x_p
\end{aligned}
\tag{2.35}
$$

where $R_c(\theta) = (I_n \otimes I_c)\cos(\theta)$ and $R_s(\theta) = (I_n \otimes I_s)\sin(\theta)$, meaning that

$$
-2x_q^T R(\theta)Q x_p = 2\alpha \cos(\theta) + 2\beta \sin(\theta)
$$

where $\alpha = -x_q^T(I_n \otimes I_c)Qx_p$ and $\beta = -x_q^T(I_n \otimes I_s)Qx_p$, from which it immediately follows that

$$J_1^*(\theta) = \alpha\cos(\theta) + \beta\sin(\theta) + \gamma \tag{2.36}$$

where $\gamma = \frac{1}{2}\left(x_p^T Q x_p + x_q^T Q x_q\right)$. By virtue of the sinusoidal form (2.36), it follows from Lemma 3 that $J_1^*(\theta)$ has a unique minimum for $\theta \in [-\pi, \pi]$ given by (2.14), which leads to the MLEs of t and μ given by (2.17) and (2.18), respectively. $\square$

Theorem 1 provides a closed form solution for maximizing the likelihood L_1 of common landmarks in the case that the covariances of p and q are of the form $\Sigma_p = \sigma_p^2 I_{2n}$ and $\Sigma_q = \sigma_q^2 I_{2n}$, respectively, and the data partitioning into common and uncommon parts is known. Specifically, given the likelihood

$$L_1(\mu, t, \theta) \triangleq \eta\exp -\frac{1}{2}J_1(\mu, t, \theta) \tag{2.37}$$

where the function J_1 is defined as

$$J_1(\mu, t, \theta) \triangleq ||x_p^1 - \mu||_{\Sigma_p^{-1}}^2 + ||x_q^1 - R(\theta)\mu - Ft||_{\Sigma_q^{-1}}^2, \tag{2.38}$$

Theorem 1 specifies the parameters μ^*, t^* and θ^* such that

$$L_1(\mu^*, t^*, \theta^*) = \max_{\mu, t, \theta} L_1(\mu, t, \theta) \tag{2.39}$$

for $\Sigma_p = \sigma_p^2 I_{2n}$ and $\Sigma_q = \sigma_q^2 I_{2n}$. An important note, however, is that $Q = 0_{2\times2}$ when $n = 1$, meaning $n > 1$ common landmarks are required to compute the solution of Theorem 1 (a minimum of $n = 3$ common landmarks are recommended).

2.4 Anisotropic approximation

An extension of the ML fusion rule (2.18) is derived by considering covariances Σ_p and Σ_q of anisotropic structure (i.e., no assumption on structure beyond the requirements of being positive definite and symmetric). In this case, least squares estimators satisfying (2.39) are no longer found in closed form due to the nonlinear parameter θ. Using the closed form solution θ^* provided by Theorem 1, least squares estimators of the parameters μ and t are derived instead to satisfy

$$L_1(\hat{\mu}, \hat{t}, \theta^*) = \max_{\mu, t} L_1(\mu, t, \theta^*) \tag{2.40}$$

resulting in a closed form approximation of the parameter μ of the form

$$\hat{\mu}(\theta^*) = \Phi_p(\theta^*) x_p^1 + \Phi_q(\theta^*) x_q^1 \tag{2.41}$$

where the fusion gains Φ_p and Φ_q are given by Algorithm 1 (see Section 2.4.1 for derivation). By deriving $\hat{\mu}$ as a a linear combination of x_p^1 and x_q^1, a combined covariance matrix is then specified as

$$\hat{\Sigma}(\theta^*) = \Phi_p(\theta^*) \Sigma_p [\Phi_p(\theta^*)]^T + \Phi_q(\theta^*) \Sigma_q [\Phi_q(\theta^*)]^T. \tag{2.42}$$

An illustration of the anisotropic approximation is shown in Fig. 2.1 in a data fusion scenario involving $n = 3$ common landmarks (the performance of the proposed fusion rules is discussed in Section 5.2). Some properties of the matrix gains Φ_p and Φ_q are provided in Section 2.4.2.
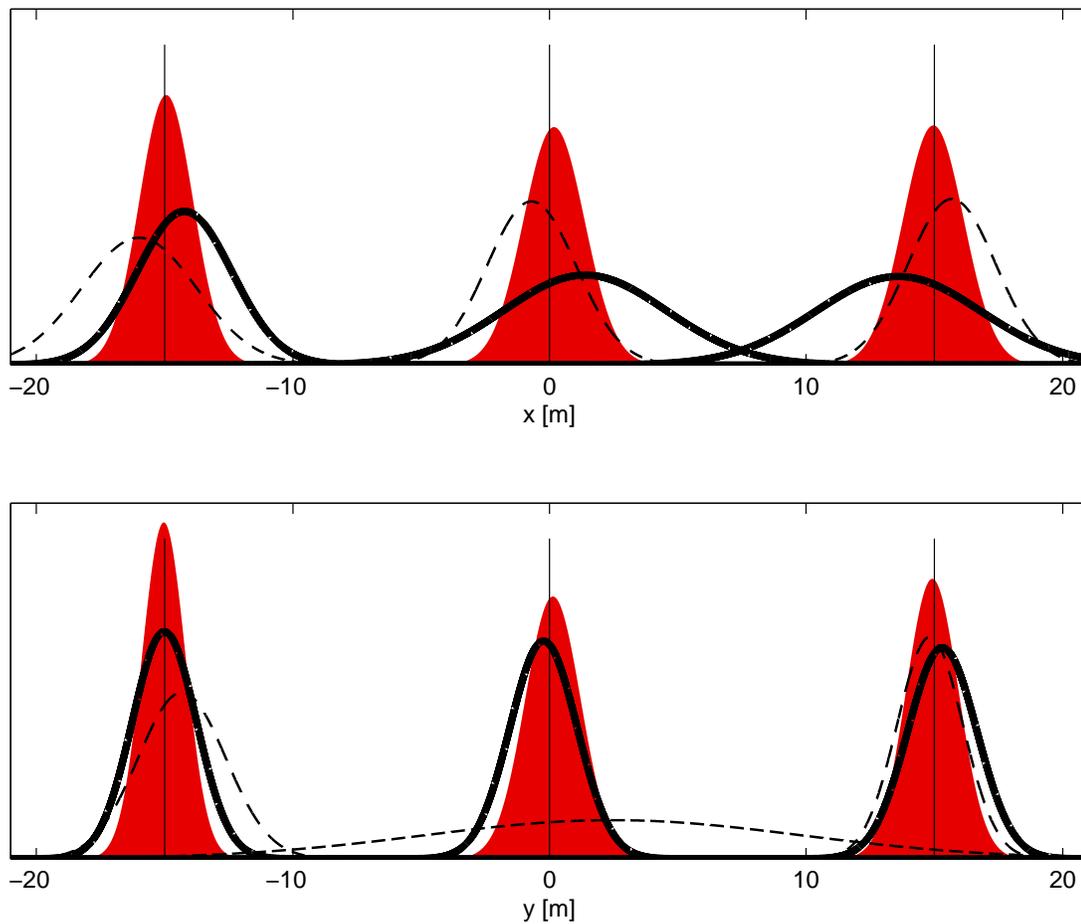
Figure 2.1: Illustration of anisotropic data fusion: (top) x and (bottom) y locations. Three landmarks (vertical black lines) located at the coordinates $(-15, -15)$, $(0, 0)$ and $(15, 15)$ are estimated individually by a fusion agent (bold lines) and a contributing agent (dashed lines). Data fusion enables the fusion agent to estimate the location of landmarks by incorporating the data of a contributing agent (illustrated in red). The peak of each distribution corresponds to the estimated landmark location, while the width indicates the uncertainty of the estimate.

Algorithm 1 Computation of $\Phi_p(\theta)$ and $\Phi_q(\theta)$

Input: Relative rotation $\theta \in [-\pi, \pi]$ and covariance matrices $\Sigma_p \in \mathbb{R}^{2n \times 2n}$ (agent p) and $\Sigma_q \in \mathbb{R}^{2n \times 2n}$ (agent q)

Output: $\Phi_p(\theta)$ and $\Phi_q(\theta)$

Application: Multi-coordinate system data fusion

1: $R(\theta) = I_n \otimes r(\theta)$

2: $\bar{\Sigma}(\theta) = \left[\Sigma_p^{-1} + R^T(\theta)\Sigma_q^{-1}R(\theta) \right]^{-1}$

3: $\Omega(\theta) = \Sigma_q^{-1} - \Sigma_q^{-1}R(\theta)\bar{\Sigma}(\theta)R^T(\theta)\Sigma_q^{-1}$

4: $F = e_n \otimes I_2$

5: $\tilde{Q}(\theta) = F(F^T\Omega(\theta)F)^{-1}F^T$

6: $\tilde{\Sigma}_q(\theta) = \Sigma_q + R(\theta)\Sigma_pR^T(\theta) - \tilde{Q}(\theta)$

7: $W(\theta) = \bar{\Sigma}(\theta)R^T(\theta)\Sigma_q^{-1}$

8: $\Phi_p(\theta) = \left[\bar{\Sigma}(\theta) + W(\theta)\tilde{Q}(\theta)W^T(\theta) \right] \Sigma_p^{-1}$

9: $\Phi_q(\theta) = W(\theta)\tilde{\Sigma}_q(\theta)W^T(\theta)\Sigma_p^{-1}R^T(\theta)$

2.4.1 Derivation of fusion gains $\Phi_p(\theta)$ and $\Phi_q(\theta)$

Given the parameter θ, the likelihood equations associated with the unknown parameters μ and t are

$$\frac{\partial \ln L_1(\mu, t, \theta)}{\partial \mu} = 0 \quad \text{and} \quad \frac{\partial \ln L_1(\mu, t, \theta)}{\partial t} = 0 \tag{2.43}$$

respectively. The estimators of μ and t that satisfy the respective likelihood equations are

$$\bar{\mu} = \bar{\Sigma}(\theta) \left[\Sigma_p^{-1}x_p + R^T(\theta)\Sigma_q^{-1}(x_q - Ft) \right] \tag{2.44}$$

where $\bar{\Sigma}(\theta) = \left[\Sigma_p^{-1} + R^T(\theta)\Sigma_q^{-1}R(\theta) \right]^{-1}$ and

$$\bar{t} = (F^T\Sigma_q^{-1}F)^{-1}F^T\Sigma_q^{-1}\left(x_q - R(\theta)\mu\right) \tag{2.45}$$

respectively. Using the expression (2.44) and the evaluation $\mu = \bar{\mu}$ in (2.45) leads to the expression

$$\hat{t} = (F^T\Omega(\theta)F)^{-1}F^T\Sigma_q^{-1}\left\{-R(\theta)\bar{\Sigma}(\theta)\Sigma_p^{-1}x_p + \left[I_{2n} - R(\theta)\bar{\Sigma}(\theta)R^T(\theta)\Sigma_q^{-1}\right]x_q\right\} \tag{2.46}$$

where $\Omega(\theta) = \Sigma_q^{-1} - \Sigma_q^{-1}R(\theta)\bar{\Sigma}(\theta)R^T(\theta)\Sigma_q^{-1}$. Using the expression (2.46) and the evaluation $t = \hat{t}$ in (2.44) leads to the expression

$$\hat{\mu}(\theta) = \bar{\Sigma}(\theta)\left\{[\Sigma_p^{-1} + R^T(\theta)K(\theta)]x_p + R^T(\theta)[\Sigma_q^{-1} - K(\theta)R^T(\theta)]x_q\right\} \tag{2.47}$$

where $K(\theta) = \Sigma_q^{-1}\tilde{Q}(\theta)\Sigma_q^{-1}R(\theta)\bar{\Sigma}(\theta)\Sigma_p^{-1}$ with $\tilde{Q}(\theta) = F(F^T\Omega(\theta)F)^{-1}F^T$. It follows that

$$\hat{\mu}(\theta) = \Gamma_p(\theta)x_p + \Gamma_q(\theta)x_q \tag{2.48}$$

where the matrix $\Gamma_p(\theta)$ is given by

$$\begin{aligned}
\Gamma_p(\theta) &= \bar{\Sigma}(\theta)\left[\Sigma_p^{-1} + R^T(\theta)K(\theta)\right] \\
&= \bar{\Sigma}(\theta)\Sigma_p^{-1} + \bar{\Sigma}(\theta)R^T(\theta)\Sigma_q^{-1}\tilde{Q}(\theta)\Sigma_q^{-1}R(\theta)\bar{\Sigma}(\theta)\Sigma_p^{-1} \\
&= \left[\bar{\Sigma}(\theta) + \bar{\Sigma}(\theta)R^T(\theta)\Sigma_q^{-1}\tilde{Q}(\theta)\Sigma_q^{-1}R(\theta)\bar{\Sigma}(\theta)\right]\Sigma_p^{-1} \\
&= \left[\bar{\Sigma}(\theta) + W(\theta)\tilde{Q}(\theta)W^T(\theta)\right]\Sigma_p^{-1} \\
&= \Phi_p(\theta)
\end{aligned}$$

where $W(\theta) = \bar{\Sigma}(\theta)R^T(\theta)\Sigma_q^{-1}$ and $\Phi_p(\theta) = \left[\bar{\Sigma}(\theta) + W(\theta)\tilde{Q}(\theta)W^T(\theta)\right]\Sigma_p^{-1}$ and the matrix $\Gamma_q(\theta)$ is given by

$$
\begin{aligned}
\Gamma_q(\theta) &= \bar{\Sigma}(\theta)R^T(\theta)\left[\Sigma_q^{-1} - K(\theta)R^T(\theta)\right] \\
&= \bar{\Sigma}(\theta)R^T(\theta)\left[\Sigma_q^{-1} - \Sigma_q^{-1}\tilde{Q}(\theta)\Sigma_q^{-1}R(\theta)\bar{\Sigma}(\theta)\Sigma_p^{-1}R^T(\theta)\right] \\
&= \bar{\Sigma}(\theta)R^T(\theta)\Sigma_q^{-1}\left[I_{2n} - \tilde{Q}(\theta)\Sigma_q^{-1}R(\theta)\bar{\Sigma}(\theta)\Sigma_p^{-1}R^T(\theta)\right] \\
&= \bar{\Sigma}(\theta)R^T(\theta)\Sigma_q^{-1}\left[R(\theta)\Sigma_p(\theta)\bar{\Sigma}^{-1}(\theta)R^T(\theta)\Sigma_q - \tilde{Q}(\theta)\right]\Sigma_q^{-1}R(\theta)\bar{\Sigma}(\theta)\Sigma_p^{-1}R^T(\theta) \\
&= W(\theta)\left[R(\theta)\Sigma_p(\theta)\bar{\Sigma}^{-1}(\theta)R^T(\theta)\Sigma_q - \tilde{Q}(\theta)\right]W^T(\theta)\Sigma_p^{-1}R^T(\theta) \\
&= W(\theta)\left\{R(\theta)\Sigma_p(\theta)\left[\Sigma_p^{-1} + R^T(\theta)\Sigma_q^{-1}R(\theta)\right]R^T(\theta)\Sigma_q - \tilde{Q}(\theta)\right\}W^T(\theta)\Sigma_p^{-1}R^T(\theta) \\
&= W(\theta)\left[\Sigma_q + R(\theta)\Sigma_p R^T(\theta) - \tilde{Q}(\theta)\right]W^T(\theta)\Sigma_p^{-1}R^T(\theta) \\
&= W(\theta)\tilde{\Sigma}_q(\theta)W^T(\theta)\Sigma_p^{-1}R^T(\theta) \\
&= \Phi_q(\theta)
\end{aligned}
$$

where $\tilde{\Sigma}_q(\theta) = \Sigma_q + R(\theta)\Sigma_p R^T(\theta) - \tilde{Q}(\theta)$ and $\Phi_q(\theta) = W(\theta)\tilde{\Sigma}_q(\theta)W^T(\theta)\Sigma_p^{-1}R^T(\theta)$.

2.4.2 Properties of $\Phi_p(\theta)$ and $\Phi_q(\theta)$

The following properties of $\Phi_p(\theta)$ and $\Phi_q(\theta)$ are considered.

1. Property 1 states that the anisotropic approximation provided by (2.41) yields the closed form solution (2.18) in the case that the Σ_p and Σ_q are isotropic in structure.

2. Given that the data provided by each agent is obtained in separate coordinate systems, it follows that a single landmark does not provide sufficient context for constructing a combined map. Property 2 thus states that in the case of

a single common landmark, the fusion agent p will retain its own landmark estimate and ignore the data provided by the contributor q. A meaningful application of data fusion in multiple coordinate systems therefore requires the data to contain $n > 1$ common landmarks.

3. In the case that the coordinate systems of the agents are the same (and in fact, for arbitrary t), Property 3 states that the data fusion rules provided by (2.18) and (2.41) yield an *affine combination* of the common landmarks x_p^1 and x_q^1. In the general case of multiple coordinate systems, however, the proposed fusion rules specify a linear combination of the data provided by each agent.

Property 1 *If $\Sigma_p = \sigma_p^2 I_{2n}$ and $\Sigma_q = \sigma_q^2 I_{2n}$, respectively, then $\Phi_p(\theta^*) = \phi_p^*$ and $\Phi_q(\theta^*) = \phi_q^*$.*

Proof: Using the simplifications of $\bar{\Sigma}(\theta)$, $\tilde{Q}(\theta)$ and $W(\theta)$ given by

$$
\begin{aligned}
\bar{\Sigma}(\theta) &= \frac{\sigma_p^2 \sigma_q^2}{\sigma_p^2 + \sigma_q^2} I_{2n} \\
\tilde{Q}(\theta) &= (\sigma_p^2 + \sigma_q^2)\bar{Q} \\
W(\theta) &= \frac{\sigma_p^2}{\sigma_p^2 + \sigma_q^2} R^T(\theta)
\end{aligned}
$$

respectively, where $\bar{Q} = F(F^T F)^{-1} F^T$, it follows that

$$
\begin{aligned}
\Phi_p(\theta) &= \left[\bar{\Sigma}(\theta) + W(\theta)\tilde{Q}(\theta)W^T(\theta) \right] \Sigma_p^{-1} \\
&= \frac{\sigma_q^2}{\sigma_p^2 + \sigma_q^2} I_{2n} + \frac{\sigma_p^2}{\sigma_p^2 + \sigma_q^2} \bar{Q} \\
&= I_{2n} - \frac{\sigma_p^2}{\sigma_p^2 + \sigma_q^2} Q
\end{aligned}
$$

Since $\tilde{\Sigma}(\theta) = (\sigma_p^2 + \sigma_q^2)Q$ when $\Sigma_p = \sigma_p^2 I_{2n}$ and $\Sigma_q = \sigma_q^2 I_{2n}$, the matrix $\Phi_q(\theta)$ reduces to

$$\Phi_q(\theta) = W(\theta)\tilde{\Sigma}_q(\theta)W^T(\theta)\Sigma_p^{-1}R^T(\theta)$$

$$= \frac{\sigma_p^2}{\sigma_p^2+\sigma_q^2}QR^T(\theta)$$

so that $\Phi_p(\theta) = I_{2n} - \frac{\sigma_p^2}{\sigma_p^2+\sigma_q^2}Q$ and $\Phi_q(\theta) = \frac{\sigma_p^2}{\sigma_p^2+\sigma_q^2}QR^T(\theta)$. $\quad\square$

Property 2 If $n = 1$, then $\Phi_p(\theta) = I_2$ and $\Phi_q(\theta) = 0_{2\times2}$ for $\theta \in [-\pi, \pi]$.

Proof: Since $\tilde{Q}(\theta) = \Sigma_q + R(\theta)\Sigma_p R^T(\theta)$ when $n = 1$, it follows that

$$\tilde{\Sigma}_q(\theta) = \Sigma_q + R(\theta)\Sigma_p R^T(\theta) - \tilde{Q}(\theta)$$

$$= \Sigma_q + R(\theta)\Sigma_p R^T(\theta) - [\Sigma_q + R(\theta)\Sigma_p R^T(\theta)]$$

$$= 0_{2\times2}$$

so that $\Phi_p(\theta)$ reduces as

$$\Phi_p(\theta) = [\bar{\Sigma}(\theta) + W(\theta)\tilde{Q}(\theta)W^T(\theta)]\Sigma_p^{-1}$$

$$= [\bar{\Sigma}(\theta) + \Sigma_p - \bar{\Sigma}(\theta)]\Sigma_p^{-1}$$

$$= I_2.$$

Since $\tilde{\Sigma}_q(\theta) = 0_{2\times2}$ when $n = 1$, $\Phi_q(\theta)$ reduces as

$$\Phi_q(\theta) = W(\theta)\tilde{\Sigma}_q(\theta)W^T(\theta)\Sigma_p^{-1}R^T(\theta)$$

$$= W(\theta)[0_{2\times2}]W^T(\theta)\Sigma_p^{-1}R^T(\theta)$$

$$= 0_{2\times2}$$

meaning $\Phi_p(\theta) = I_2$ and $\Phi_q(\theta) = 0_{2\times2}$ when $n = 1$. $\quad\square$

Property 3 *If $\theta = 0$, $\Phi_p(0) + \Phi_q(0) = I_{2n}$.*

Proof: Using $\Phi_p(\theta)$ and $\Phi_q(\theta)$ provided in Algorithm 1 and the equivalent form of $\tilde{\Sigma}_q(\theta)$ when $\theta = 0$ given by

$$
\begin{aligned}
\tilde{\Sigma}_q(0) &= \Sigma_q + R(0)\Sigma_p R^T(0) - \tilde{Q}(0) \\
&= \Sigma_q + \Sigma_p - \tilde{Q}(0)
\end{aligned}
$$

it follows that $\Phi_p(0)$ and $\Phi_q(0)$ are then

$$
\Phi_p(0) = \left[\bar{\Sigma}(0) + W(0)\tilde{Q}(0)W^T(0) \right] \Sigma_p^{-1}
$$

and

$$
\begin{aligned}
\Phi_q(0) &= W(0)\tilde{\Sigma}_q(0)W^T(0)\Sigma_p^{-1}R^T(0) \\
&= W(0)\left[\Sigma_q + \Sigma_p - \tilde{Q}(0) \right] W^T(0)\Sigma_p^{-1}
\end{aligned}
$$

respectively. The sum of $\Phi_p(0)$ and $\Phi_q(0)$ is then

$$
\begin{aligned}
\Phi_p(0) + \Phi_q(0) &= \bar{\Sigma}(0)\Sigma_p^{-1} + W(0)\left(\Sigma_p + \Sigma_q \right)W^T(0)\Sigma_p^{-1} \\
&= \left[\bar{\Sigma}(0) + W(0)\left(\Sigma_p + \Sigma_q \right)W^T(0) \right]\Sigma_p^{-1}.
\end{aligned}
$$

However, since $W(0) = \bar{\Sigma}(0)R^T(0)\Sigma_q^{-1} = \bar{\Sigma}(0)\Sigma_q^{-1}$ when $\theta = 0$, it follows that

$$
\begin{aligned}
\Phi_p(0) + \Phi_q(0) &= \left[\bar{\Sigma}(0) + W(0)\left(\Sigma_p + \Sigma_q \right)W^T(0) \right]\Sigma_p^{-1} \\
&= \left[\bar{\Sigma}(0) + \Sigma_p - \bar{\Sigma}(0) \right]\Sigma_p^{-1} \\
&= [\Sigma_p]\Sigma_p^{-1} \\
&= I_{2n}
\end{aligned}
$$

which proves that $\Phi_p(0) + \Phi_q(0) = I_{2n}$. $\qquad\square$

CHAPTER 3

CRAMÉR-RAO BOUNDS OF MODEL PARAMETERS

3.1 Introduction

This chapter derives benchmark performance bounds known as the *Cramér-Rao lower bounds* [27, 28, 29, 30] for the maximum likelihood estimators proposed in Theorem 1. The bounds are derived by applying the following theorem in the case of Gaussian model.

Theorem 2 *Suppose that a random variable X has an n-variate Gaussian distribution with a probability density function parameterized by ϕ as*

$$p_X(x;\phi) = \frac{1}{\sqrt{(2\pi)^n|\Sigma(\phi)|}} \exp -\frac{1}{2}[x - m(\phi)]^T\Sigma^{-1}(\phi)[x - m(\phi)], \qquad (3.1)$$

then the entries of the Fisher information matrix $I(\phi)$ are given by

$$
\begin{aligned}
I_{ij}(\phi) \;=\; & \left[\frac{\partial m(\phi)}{\partial \phi_i}\right]^T \Sigma^{-1}(\phi) \left[\frac{\partial m(\phi)}{\partial \phi_j}\right] \\
& + \frac{1}{2}\,\mathrm{trace}\left\{\Sigma^{-1}(\phi)\left[\frac{\partial m(\phi)}{\partial \phi_i}\right]^T \Sigma^{-1}(\phi)\left[\frac{\partial m(\phi)}{\partial \phi_j}\right]\right\}
\end{aligned}
\qquad (3.2)
$$

so that $I(\phi) = [I_{ij}(\phi)]$.

Proof: See Kay [31], App. 3C.   □

3.2 Gaussian Cramér-Rao lower bounds

Consider the Gaussian model of n points (referred to as landmarks) given by the random variable of the form

$$X \sim \mathcal{N}\left(m(\phi), \Sigma(\phi)\right) \tag{3.3}$$

with model parameters $\phi = (\mu^T, t^T, \theta^T)^T$ consisting of the (x, y)-coordinates $\mu \in \mathbb{R}^{2n}$, the rotation angle $\theta \in [-\pi, \pi]$ and the translation parameter $t \in \mathbb{R}^2$. The deterministic, but unknown, mean of (3.3) is partitioned into two parts, corresponding to coordinates systems p and q, as

$$m(\phi) = \begin{pmatrix} \mu \\ R(\theta)\mu + Ft \end{pmatrix} \tag{3.4}$$

with covariance $\Sigma(\phi) = \sigma^2 I_{4n}$. Under this model, the entries of the *Fisher information matrix* [31] $I(\phi) = [I_{ij}(\phi)]$ are given by

$$I_{ij}(\phi) = \frac{1}{\sigma^2} \left[\frac{\partial m(\phi)}{\partial \phi_i}\right]^T \left[\frac{\partial m(\phi)}{\partial \phi_j}\right] \tag{3.5}$$

which are computed from the partial derivatives of $m(\phi)$ with respect to the model parameters. In vector form, the partial derivatives are given by

$$D_\mu = \frac{\partial m(\phi)}{\partial \mu} = \begin{pmatrix} I_{2n} \\ R(\theta) \end{pmatrix} \tag{3.6}$$

$$D_t = \frac{\partial m(\phi)}{\partial t} = \begin{pmatrix} 0_{2n \times 2} \\ F \end{pmatrix} \tag{3.7}$$

$$D_\theta = \frac{\partial m(\phi)}{\partial \theta} = \begin{pmatrix} 0_{2n \times 1} \\ R(\theta) L_s^T \mu \end{pmatrix} \tag{3.8}$$

with $L_s = I_n \otimes \begin{pmatrix} 0 & -1 \\ 1 & 0 \end{pmatrix}$, which leads to the Fisher information matrix

$$I(\phi) = \frac{1}{\sigma^2} \begin{pmatrix} D_\mu^T D_\mu & D_\mu^T D_t & D_\mu^T D_\theta \\ D_t^T D_\mu & D_t^T D_t & D_t^T D_\theta \\ D_\theta^T D_\mu & D_\theta^T D_t & D_\theta^T D_\theta \end{pmatrix}$$

$$= \frac{1}{\sigma^2} \begin{pmatrix} 2I_{2n} & R^T(\theta)F & L_s^T \mu \\ F^T R(\theta) & F^T F & F^T R(\theta)L_s^T \mu \\ \mu^T L_s & \mu^T L_s R^T(\theta)F & \mu^T \mu \end{pmatrix}. \tag{3.9}$$

Using the matrix (3.9), the Cramér-Rao lower bound (CRLB) covariance of the model parameter ϕ is then $P(\phi) = I^{-1}(\phi)$, which leads to the following theorem concerning the performance bounds of the entries of ϕ.

Theorem 3 *The Cramér-Rao lower bounds (CRLBs) of the parameters $\{\mu, t, \theta\}$ are given by the following expressions.*

1. *The CRLB of the rotation parameter θ is*

$$P_{\theta,\theta} = \sigma^2 \frac{1}{\zeta} \tag{3.10}$$

   where $\zeta = \frac{1}{2}\mu^T Q\mu$ and $Q = I_{2n} - F(F^T F)^{-1}F^T$.

2. *The CRLB of the parameter μ is*

$$P_{\mu,\mu} = \sigma^2 \left(U + \frac{1}{\zeta}uu^T \right) \tag{3.11}$$

   where $U = I_{2n} - \frac{1}{2}Q$ and $u = \frac{1}{2}QL_s^T\mu$.

3. The CRLB of the translation t is

$$P_{t,t} = \sigma^2 \left(V + \frac{1}{\zeta} v v^T \right) \tag{3.12}$$

where $V = \frac{2}{n} I_2$ *and* $v = \frac{1}{n} F^T R(\theta) L_s^T \mu$.

Proof: The CRLBs of the model parameters $\{\mu, t, \theta\}$ are determined by considering the block partitioning of the Fisher information matrix (3.9) of the form

$$I(\phi) = \frac{1}{\sigma^2} \begin{pmatrix} A & b \\ b^T & c \end{pmatrix} \tag{3.13}$$

where A, b and c are given by

$$A = \begin{pmatrix} 2I_{2n} & R^T(\theta)F \\ F^T R(\theta) & F^T F \end{pmatrix}, \quad b = \begin{pmatrix} L_s^T \mu \\ F^T R(\theta) L_s^T \mu \end{pmatrix}$$

and $c = \mu^T \mu$, respectively. The inverse Fisher information matrix $I^{-1}(\phi)$ is computed from the inverse of A, which is determined by using the matrix

$$B = \begin{pmatrix} I_{2n} & 0_{2n \times 2} \\ -\frac{1}{2} F^T R(\theta) & I_2 \end{pmatrix} \tag{3.14}$$

to decompose A into a block diagonal form (known as the *Aitken block-diagonalization*) given by

$$\widetilde{A} = BAB^T$$
$$= \begin{pmatrix} 2I_{2n} & \\ & \frac{1}{2} F^T F \end{pmatrix}. \tag{3.15}$$

Using the relation $F^T F = n I_2$, it follows that the inverse of the matrix A is computed as

$$
\begin{aligned}
A^{-1} &= \left(B^{-1} \widetilde{A} \left[B^T \right]^{-1} \right)^{-1} \\
&= B^T \widetilde{A}^{-1} B \\
&= \begin{pmatrix} U & -\frac{1}{n} R^T(\theta) F \\ -\frac{1}{n} F^T R(\theta) & V \end{pmatrix}
\end{aligned}
\tag{3.16}
$$

where $U = I_{2n} - \frac{1}{2} Q$ and $V = \frac{2}{n} I_2$. Using the inversion formula provided in [32] and the expression of A^{-1} given by (3.16), it follows that the inverse of (3.13) is computed as

$$
\begin{aligned}
I^{-1}(\phi) &= \sigma^2 \left(\begin{array}{c|c} A^{-1} + \frac{1}{\zeta} A^{-1} b b^T A^{-1} & -\frac{1}{\zeta} A^{-1} b \\ \hline -\frac{1}{\zeta} b^T A^{-1} & \frac{1}{\zeta} \end{array} \right) \\
&= \sigma^2 \begin{pmatrix} P_{\mu,\mu} & P_{\mu,t} & P_{\mu,\theta} \\ P_{t,\mu} & P_{t,t} & P_{t,\theta} \\ P_{\theta,\mu} & P_{\theta,t} & P_{\theta,\theta} \end{pmatrix}
\end{aligned}
\tag{3.17}
$$

where $\zeta = c - b^T A^{-1} b = \frac{1}{2} \mu^T Q \mu$ and the covariances $P_{\mu,\mu}$, $P_{t,t}$ and $P_{\theta,\theta}$ are given by (3.11), (3.12) and (3.10), respectively. $\qquad \square$

The performance of the closed-form ML estimators given in Theorem 1 relative to the Cramér-Rao bounds of Theorem 3 is shown in Fig. 3.1.
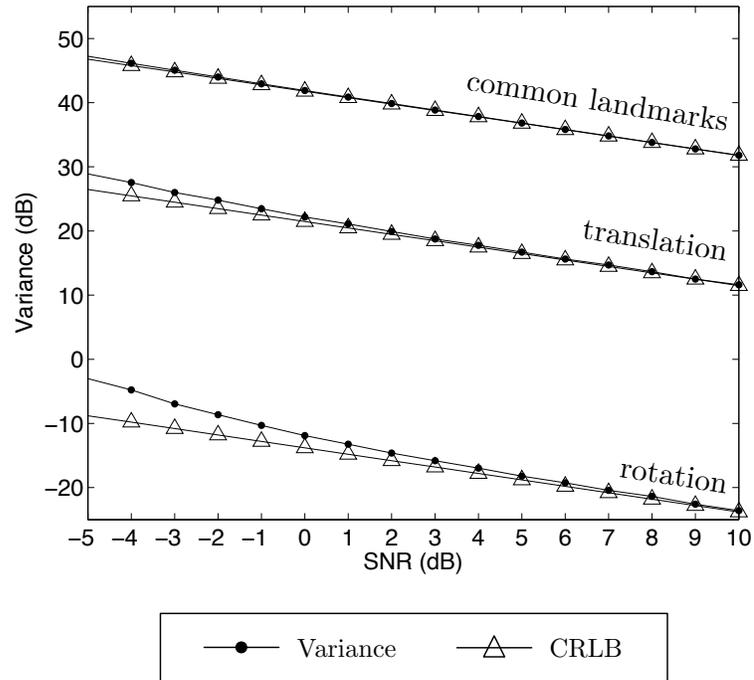
Figure 3.1: Cramér-Rao lower bounds and performance of closed-form MLE. (top) A plot of the trace of the CRLB covariance matrices $P_{\mu,\mu}$, $P_{t,t}$ and $P_{\theta,\theta}$ derived from the parameters μ (common landmarks), t (translation) and θ (rotation), respectively, is shown above in the figure. The plots are shown against the variance of the closed-form ML estimators μ^*, t^* and θ^*.

CHAPTER 4

GENERALIZED LIKELIHOOD DATA REGISTRATION

In a general mapping scenario, the ground truth structure observed by the agents is unknown. In particular, if the first two entries of $X_p = x_p$ correspond to the particular landmark, then the first two entries of $X_q = x_q$ correspond to a different landmark in general (and likewise with the remaining entries). Common landmarks in this case are identified by applying a matching procedure to x_p and x_q with consideration that the stochastic maps are obtained in separate coordinate systems related by θ and t. The matching procedure proposed in this section is based on the use of landmark triplets referred to as *triangles*, which requires that the maps of each agent contain at least three landmarks. An overview of the registration approach is shown in Fig. 4.1.

4.1 Directed hypergraph model

Triangles are constructed from the maps of each agent by following a direction convention used in the star-pattern matching approach of Groth [24]. In particular, given three landmark locations $y_a, y_b, y_c \in \mathbb{R}^2$, the Groth representation of a directed triangle is $y = (y_a^T, y_b^T, y_c^T)^T$, which is a vector in $\mathbb{R}^6$ with entries that follow the inequality

$$||y_a - y_b|| < ||y_b - y_c|| < ||y_c - y_a|| \tag{4.1}$$

under the assumption that no two triangle edges have the same length. This convention, which is invariant to changes in rotation and translation is used to construct the *directed hypergraphs* $G_p = (V_p, E_p)$ and $G_q = (V_q, E_q)$ from the Delaunay triangulations of maps p and q, respectively. The landmarks that form

(coordinate system p)　　　　　　　(coordinate system q)

Directed hypergraph model

Likelihood matrix Δ

Matching and outlier rejection
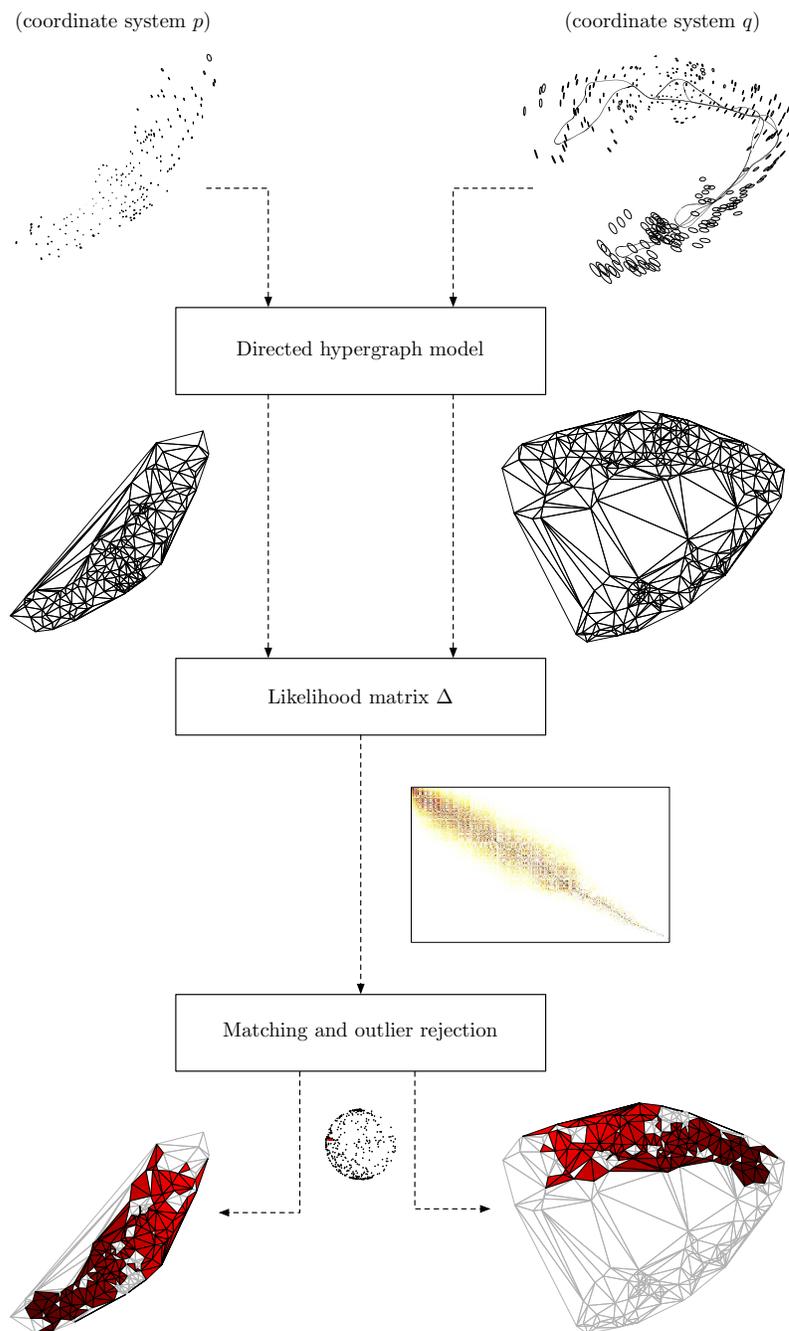
Figure 4.1: Overview of data registration approach. Common landmarks and rigid-body transform parameters are determined using a directed hypergraph representation of metric maps. Likelihood statistics of common directed triangles are stored in a matrix Δ, which is used to determine common landmarks by solving a linear assignment problem. The solution of the assignment problem is partitioned into inliers and outliers using a quaternion outlier rejection approach.

the vertices of each graph are contained by V_p (agent p) and V_q (agent q). The resulting directed triangles constructed from the maps of p and q are contained by the hyperedges E_p and E_q, respectively, with each directed triangle being indexed in order of increasing perimeter.

4.2 Hypergraph hypothesis testing

Determining common landmarks from the directed triangles of G_p and G_q is considered as a binary hypothesis testing problem. Under hypothesis H_0, the agents observe the ground truth directed triangles $\nu_p, \nu_q \in \mathbb{R}^6$, which contain a maximum of two landmarks in common. Under hypothesis H_1, the agents observe a common directed triangle $\delta \in \mathbb{R}^6$ within their respective coordinate systems. In this way, H_0 is the hypothesis of uncommon triangles and H_1 is the hypothesis of common triangles. The mathematical models of H_0 and H_1 are given by

$$
H_0 : \begin{bmatrix} Y_p \\ Y_q \end{bmatrix} \sim \mathcal{N} \left(\begin{bmatrix} \nu_p \\ \nu_q \end{bmatrix}, \begin{bmatrix} \sigma_p^2 I & \\ & \sigma_q^2 I \end{bmatrix} \right) \tag{4.2}
$$

$$
H_1 : \begin{bmatrix} Y_p \\ Y_q \end{bmatrix} \sim \mathcal{N} \left(\begin{bmatrix} \delta \\ R(\theta)\delta + Ft \end{bmatrix}, \begin{bmatrix} \sigma_p^2 I & \\ & \sigma_q^2 I \end{bmatrix} \right) \tag{4.3}
$$

respectively. The appropriate matching hypothesis (i.e., H_0 or H_1) for the directed triangle data $Y_p = y_p$ and $Y_q = y_q$ is initially unknown. Given the realizations y_p and y_q from the stochastic maps of p and q, respectively, the matching hypothesis is determined using a *generalized likelihood ratio test (GLRT)* of the form

$$
\Lambda(y_p, y_q) = \frac{\max\limits_{\delta, t, \theta} L_1(\delta, t, \theta)}{\max\limits_{\nu_p, \nu_q} L_0(\nu_p, \nu_q)} \underset{H_0}{\overset{H_1}{\gtrless}} \tau \tag{4.4}
$$
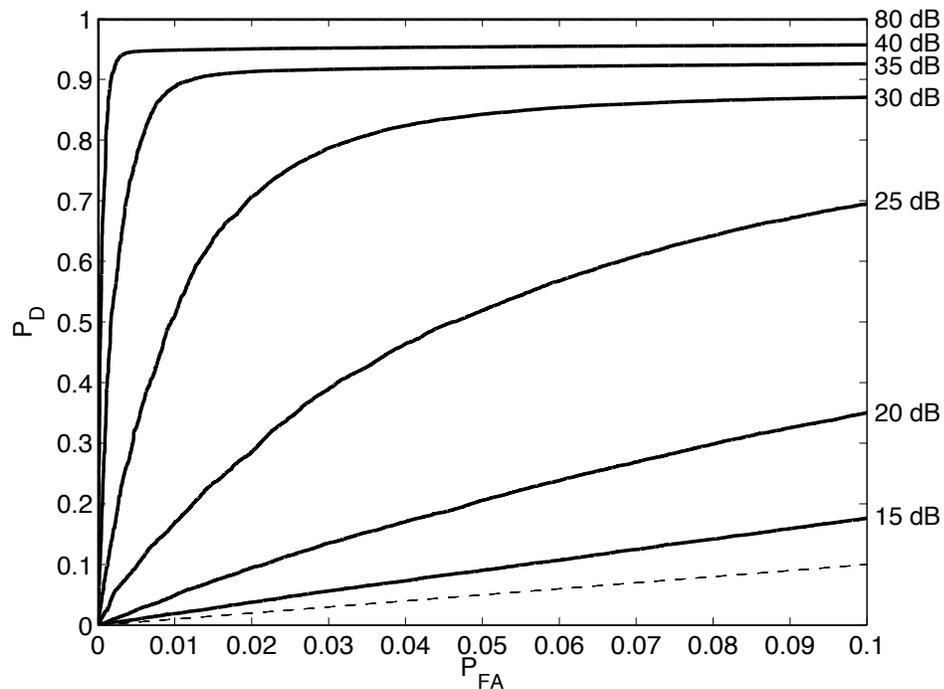
Figure 4.2: Monte Carlo performance of hypergraph hypothesis testing. Receiver operating characteristic (ROC) curves, illustrated above, show the performance of the detecting triangle matches at various levels of SNR. Each of the curves are plots of the probability of detecting a match (P_D) versus the probability of a false alarm (P_{FA}). The dashed line in the lower region of the figure indicates the performance of a random guess.

where L_k are likelihood functions under H_k, with $k \in \{0, 1\}$, and the threshold τ is selected to control the level of false alarm. The likelihood statistic $\Lambda(y_p, y_q)$ is easily computed by applying Theorem 1. The performance of the approach in the presence of noise, as illustrated by the receiver operating characteristic (ROC) curves of Fig. 4.2, is of interest due to the uncertain nature of stochastic maps. As illustrated in the figure, the performance of the approach degrades gracefully with increasing noise (the signal-to-noise ratio, or SNR, is discussed in Section 5).

4.3 Data registration and environment structure

4.3.1 Natural vs. semi-structured environments

A desirable trait of any data fusion approach is the ability to maintain performance in a variety environments and with different types of sensors. Data obtained from two types of environments and sensors are considered in this section, each of which are illustrated in Fig. 4.3. A natural environment with data obtained from a laser sensor is shown in Fig. 4.3a. In such an environment, natural landmarks such as trees are used to build a rigid-body model from data. In contrast, a semi-structured environment with data obtained from a camera sensor is shown in Fig. 4.3b. Landmarks such as edges and corner points usually aid in the construction of metric maps in environments of this type. While the data fusion approach of this paper makes no assumption on the type of sensor or environment, the benchmark datasets are used to show the potential application of the approach to rigid-body data generated from a wide range of environments and sensors. The simulated examples of Fig. 4.4 illustrate two classes of landmark arrangements related to the experimental examples of Fig. 4.3. From a registration perspective, the arrangement of landmarks in the Victoria Park example (Fig. 4.3a) resembles samples drawn from a uniform distribution (Fig. 4.4a) and landmarks in the DLR example (Fig. 4.3b) resemble landmarks arranged in a deterministic grid with additive noise (Fig. 4.4b).

(a)
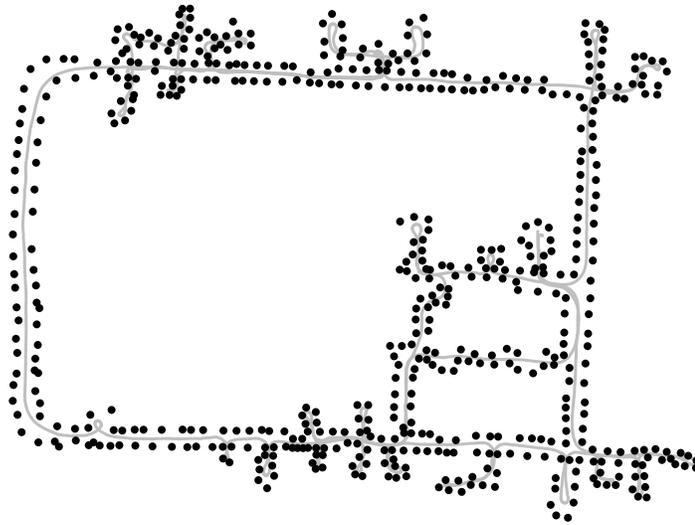
(b)

Figure 4.3: Benchmark rigid-body models of natural and semi-structured environments. (a) Victoria Park provides an example of a natural outdoor environment (dataset courtesy of the University of Sydney). Landmark locations in the environment are determined using a laser range finder. (b) An example of a semi-structured indoor environment is provided by the DLR Institute of Robotics and Mechatronics building (dataset courtesy of the University of Bremen). In contrast to the Victoria Park dataset, a camera sensor is used to determine the locations of landmarks within a research facility.
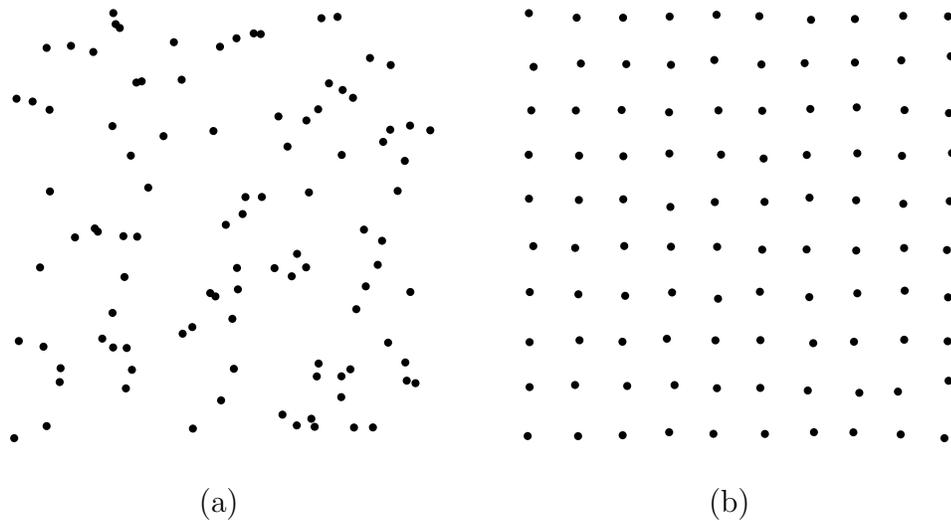
Figure 4.4: Synthetic models of natural and semi-structured environments. (a) Samples drawn from a uniform distribution provide a model of landmarks within a natural environment. (b) Landmarks in a semi-structured environment are modeled in this example by points in a deterministic grid with additive noise. Each of the examples provide simple models of the spatial arrangement of landmarks in different types of environments.

4.3.2 Hypergraph registration

An illustration of the hypergraph model as it relates to data registration is shown in Fig. 4.5. The figure illustrates the determination of common landmarks by identifying common directed triangles across the coordinate systems of each hypergraph. Using Theorem 1, a metric for determining whether a triangle $y_p \in E_p$ in hypergraph G_p corresponds to a triangle $y_q \in E_q$ in hypergraph G_q is given by the likelihood statistic

$$\Lambda(y_p, y_q) = \frac{\max\limits_{\delta, t, \theta} L_1(\delta, t, \theta)}{\max\limits_{\nu_p, \nu_q} L_0(\nu_p, \nu_q)} \tag{4.5}$$

where the parameter $\delta \in \mathbb{R}^6$ is the location of the common triangle and the parameters $\nu_p, \nu_q \in \mathbb{R}^6$ are the locations of uncommon triangles. The metric is computed

in closed form from y_p and y_q as specified by Theorem 1 since

$$\max_{\delta,t,\theta} L_1(\delta, t, \theta) = L_1(\delta^*, t^*, \theta^*) \tag{4.6}$$

under the hypothesis that y_p and y_q correspond to a common directed triangle
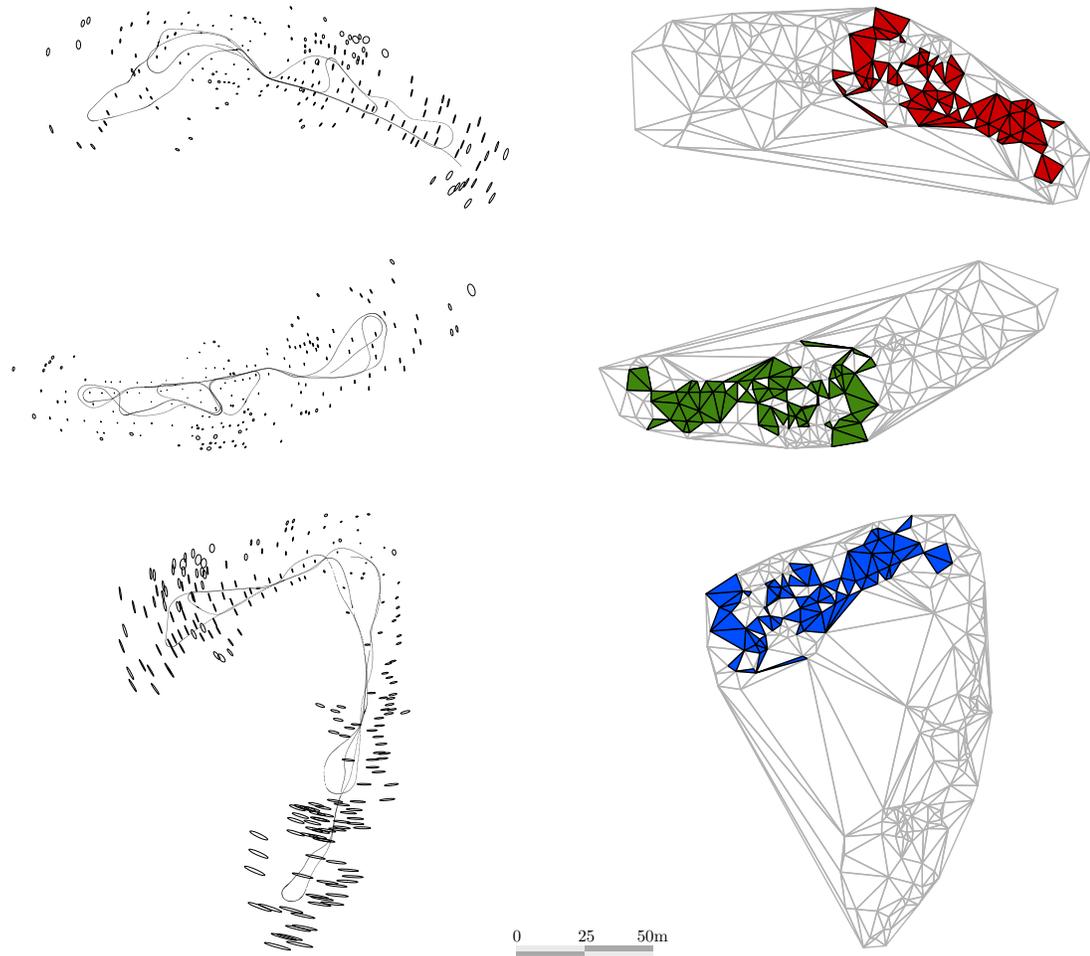
Figure 4.5: Application of directed hypergraph model to data registration. (left) Illustrated in the figure are rigid-body models of a natural environment shown in three separate coordinate systems. (right) Common landmarks represented in different coordinate systems are determined by matching directed triangles constructed from Delaunay triangulations (common directed hyperedges are illustrated by the shaded triangles). Once common triangles are determined between each hypergraph, rotation and translation parameters are estimated in closed form using the vertices of the matched triangles.

parameter δ and

$$\max_{\nu_p, \nu_q} L_0(\nu_p, \nu_q) = L_0(\nu_p^*, \nu_q^*) \tag{4.7}$$

under the hypothesis that y_p and y_q correspond to two separate directed triangle parameters ν_p and ν_q, respectively (in the later case, y_p and y_q contain only two common landmarks at best and no common landmarks in general). Likelihood statistics computed from G_p and G_q, as specified by (4.5), are stored in matrix form as $\Delta = [f_{ij}(y_p^i, y_q^j)]$ with entries

$$f_{ij}(y_p^i, y_q^j) = \begin{cases} \Lambda(y_p^i, y_q^j) & , \; i \in \mathcal{P} \text{ and } j \in \mathcal{Q} \\ 0 & , \; o.w. \end{cases} \tag{4.8}$$

where $\mathcal{P} = \{1, 2, \ldots, |E_p|\}$ and $\mathcal{Q} = \{1, 2, \ldots, |E_q|\}$. Constructing the matrix Δ from the directed triangles of G_p and G_q leads to a *linear assignment problem* [33, 34] of the form

$$\text{maximize} \quad \sum_{i=1}^{m} \sum_{j=1}^{m} f_{ij}(y_p^i, y_q^j) z_{ij} \tag{4.9}$$

$$\text{subject to} \quad \sum_{i=1}^{m} z_{ij} = 1, \quad j = 1, \ldots, m \tag{4.10}$$

$$\sum_{j=1}^{m} z_{ij} = 1, \quad i = 1, \ldots, m \tag{4.11}$$

$$\text{and} \quad z_{ij} \in \{0, 1\}, \tag{4.12}$$

where $m = \max(|E_p|, |E_q|)$, which is readily solved using optimized routines such as the Jonker-Volgenant algorithm [35] by relaxing the integer program to a linear program with decision variables $z_{ij} \in [0, 1]$. An illustration of the approach using the Victoria Park and DLR benchmarks is shown in Fig. 4.6.

(a)

(b)

(c)

(d)
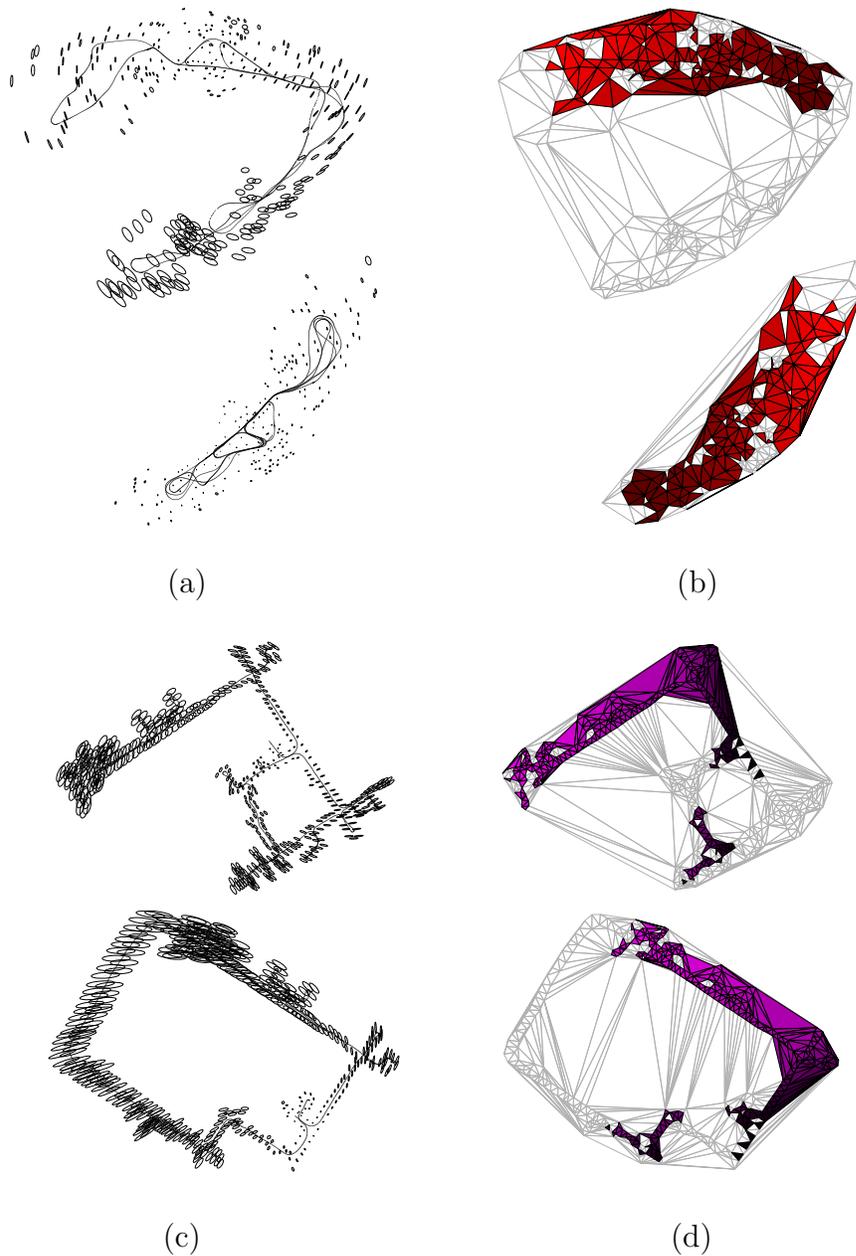
Figure 4.6: Registration of landmarks in natural and semi-structured environments. (a) Rigid-body models of the Victoria Park are shown in the coordinate systems of a fusion agent p and a contributing agent q. (b) Common landmarks are determined by solving a linear assignment problem involving directed triangles (the solution of the assignment problem is illustrated in the figure by shaded triangles with corresponding color gradients). The approach is also illustrated using the DLR dataset with rigid-body models shown in (c) and the registration solution shown in (d).

Using the solution of the assignment problem, a collection $\mathcal{C} = \{c^1, c^2, \ldots, c^m\}$ of correspondence variables is constructed to indicate m common landmarks derived from the vertices of directed triangles. Rigid-body transform parameters are then estimated by applying Theorem 1 to compute t^* and θ^* using the common landmarks indicated by $\mathcal{C}$. The data registration solution is thus of the form $\mathcal{R} = \{\mathcal{C}, t^*, \theta^*\}$, which is used to compute a combined global model using the data fusion rules proposed in Section 2.4.

An illustration of the data fusion approach and structure of the matrix Δ is shown in Fig. 4.7. The data fusion examples in the figure, which illustrate the approach using the Victoria Park and DLR benchmarks, show the combined global models within the coordinate system of the fusion agent p in addition to the likelihood structure of the explored environment. Using the directed hypergraph model, the structure of the environment (and subsequently, the complexity of the registration problem) is indicated in part by the bandedness of the likelihood matrix Δ.

4.4 Outlier rejection

The solution of the assignment problem provides a list of candidate common triangles between the hypergraphs of each agent. Associated with each triangle assignment is a maximum likelihood estimate of the parameters θ and t derived from the vertices of the triangles in order to compute the likelihood matching statistic (4.5). Under rigid body assumptions, inliers in the candidate triangle assignments are indicated by rigid-body rotation and translation parameters that form a cluster around the true values of θ (in radians) and t (in meters). A simple approach to obtain a composite representation of θ and t is to compute a *unit quaternion*

[36, 37] of the form

$$q = \left(\cos \frac{1}{2}\theta \right) + u \left(\sin \frac{1}{2}\theta \right) \tag{4.13}$$

where θ is a rotation angle about the rotation axis $u \in \mathbb{R}^3$ of unit magnitude. By

(a)

(b)
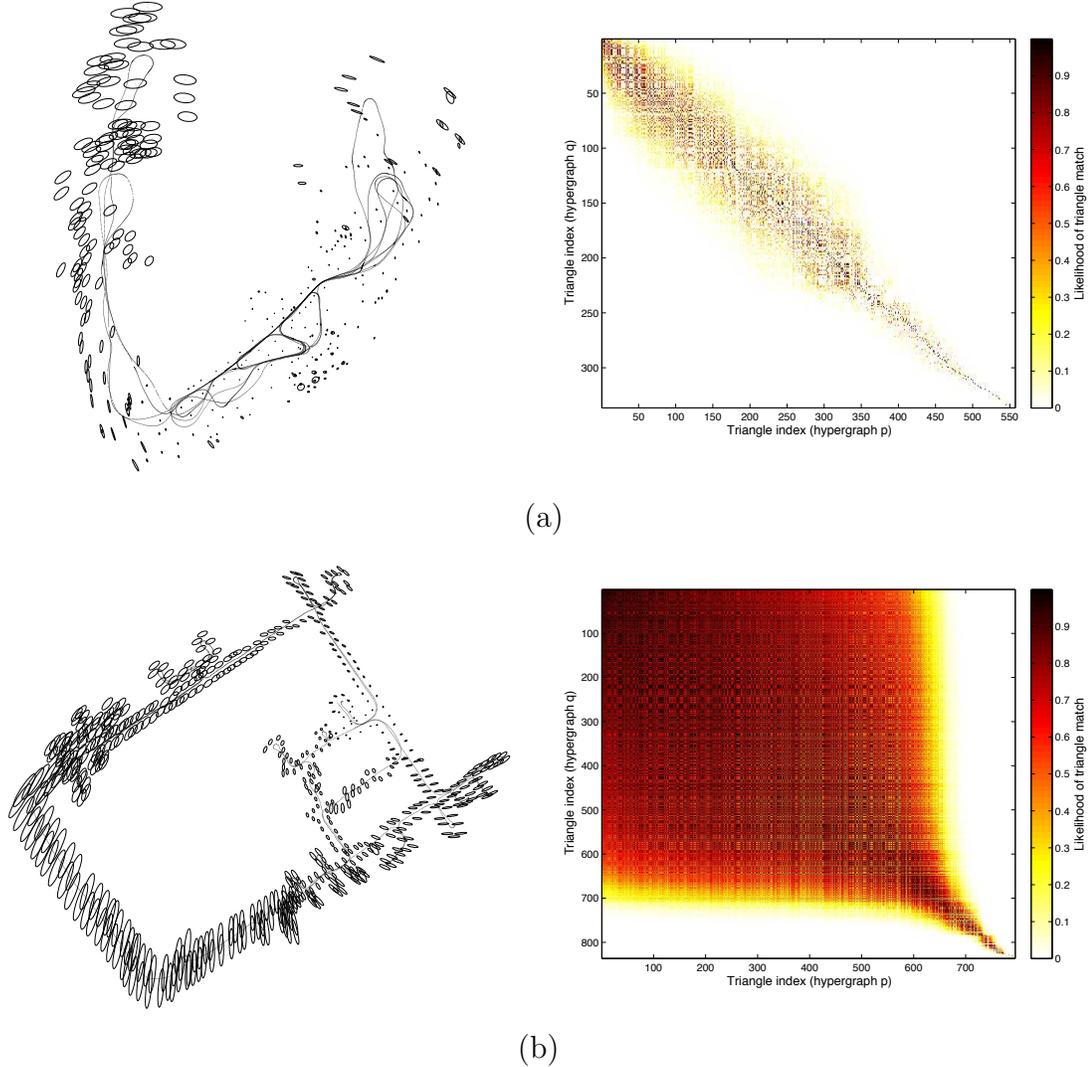
Figure 4.7: Data fusion and likelihood structure. An illustration of anisotropic data fusion in the coordinate system of a fusion agent p is shown above using the (a) Victoria Park and (b) DLR examples. The likelihood matrix Δ in each case provides an indication of the underlying structure of the environment. In contrast to the likelihood matrix of the DLR environment, the matrix Δ of the Victoria Park example naturally exhibits a banded structure.

defining the rotation axis u relative to the unit z-axis, denoted by $e_z = (0, 0, 1)^T$, a combined representation of θ and t is obtained using Algorithm 2, where the matrix $R(q)$ is a 3×3 rotation computed from the entries of $q = (q_0, q_x, q_y, q_z)^T$ as

$$
R(q) = \begin{pmatrix} q_0^2 + q_x^2 - q_y^2 - q_z^2 & 2(q_x q_y - q_0 q_z) & 2(q_x q_z + q_0 q_y) \\ 2(q_y q_x + q_0 q_z) & q_0^2 - q_x^2 + q_y^2 - q_z^2 & 2(q_y q_z - q_0 q_x) \\ 2(q_z q_x - q_0 q_y) & 2(q_z q_y + q_0 q_x) & q_0^2 - q_x^2 - q_y^2 + q_z^2 \end{pmatrix}. \quad (4.14)
$$

The resulting representation of the rigid-body transform parameters is a 3D coordinate $\rho \in \mathbb{R}^3$ on the unit sphere. Inliers in candidate triangle assignments are thus indicated by unit sphere coordinates that form a cluster around the coordinate ρ computed from the true values of θ and t. Using the spherical representation of the rigid-body transform parameters provided by Algorithm 2, inliers and outliers are detected by applying standard random sample consensus (RANSAC) [38] routines to the resulting 3D points. An illustration of the outlier rejection approach is shown in Fig. 4.8. Eliminating outliers in triangle assignments leads to a registration solution given by $\mathcal{R}^* = \{\mathcal{C}^*, t^*, \theta^*\}$, where $\mathcal{C}^* \subseteq \mathcal{C}$ is the collection of inlier correspondence variables used to compute the parameters t^* and θ^*.

Algorithm 2 Quaternion representation of θ and t

Input: Rotation parameter $\theta \in [-\pi, \pi]$ and translation $t \in \mathbb{R}^2$

Output: Unit sphere coordinate $\rho \in \mathbb{R}^3$, unit quaternion q

Application: Outlier rejection

1: $v = \begin{pmatrix} t \\ 1 \end{pmatrix}$

2: $q = \cos \dfrac{\theta}{2} + \dfrac{v}{||v||} \sin \dfrac{\theta}{2}$

3: $\rho = R(q) e_z$

(a)

(b)

(c)
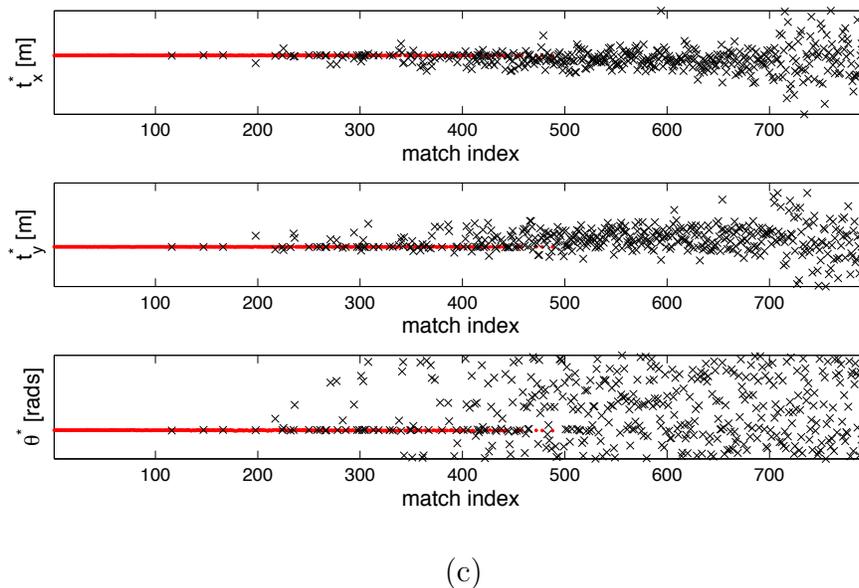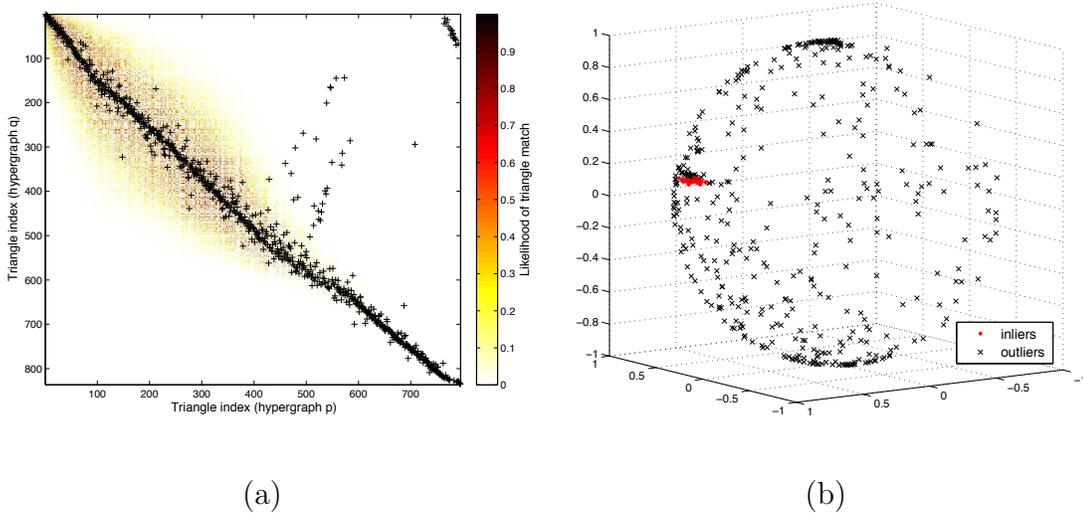
Figure 4.8: Identifying inliers and outliers in hypergraph registration. (a) Common triangles between the hypergraphs G_p and G_q, determined by solving a linear assignment problem, are indicated in the figure by black markers superimposed on a likelihood matrix Δ. (b) Each entry of the assignment solution is used to compute an estimate of the rigid body parameters t and θ, illustrated above using a quaternion representation on the unit sphere. Inliers (red dots) and outliers (black crosses) are determined by applying random sample consensus to the spherical representation. (c) For illustration purposes, the corresponding rigid-body parameters (classified as inliers and outliers) are plotted in order of decreasing likelihood statistics.

CHAPTER 5

NUMERICAL EXAMPLES AND SIMULATIONS

5.1 Victoria Park example

An illustration of the proposed ML fusion approach is shown in Fig. 5.1. The ground truth landmarks shown in the figure are obtained by applying the sparse local submap joining filter (SLSJF) proposed by Huang *et al.* [39] to the Victoria Park dataset. The ground truth is partitioned into two vectors u_p and u_q as models of the ground truth landmark locations observed by agent p and agent q, respectively (see Chapter 2). The stochastic maps of each agent are generated using the additive noise model discussed in Section 2.4 at an SNR of 30dB. The rotation (in radians) and translation (in meters) applied to the stochastic map agent q are $\theta = 0.7854$ and $t = (100, 5)^T$, respectively. As illustrated in the figure, θ and t parameterize a spatial transform of the stochastic map of agent q in reference to the ground truth coordinate frame (i.e., the coordinate system of agent p).

The directed hypergraph representation of each stochastic map is used by the GLR matching to determine the common directed triangles across the coordinate systems of the agents (using the Groth convention enables to the determination of common landmarks from common directed triangles). The number of directed triangles in hypergraphs p and q are $|E_p| = 340$ and $|E_q| = 304$, respectively. Due to the uncertainty of the stochastic maps, outlier rejection is required to determine an inlier set of matching triangles (as illustrated in Fig. 5.2). Theorem 1 is then applied to the inlier landmarks to compute the closed form MLEs $\theta^* = 0.7878$ and $t^* = (100.0860, 4.9120)^T$. Maximum likelihood estimation of the combined map $u^* = (\mu^{*T}, v_p^{*T}, v_q^{*T})^T$ immediately follows from Lemma 1 and Theorem 1.

Ground truth

Data Models

Hypergraph Registration
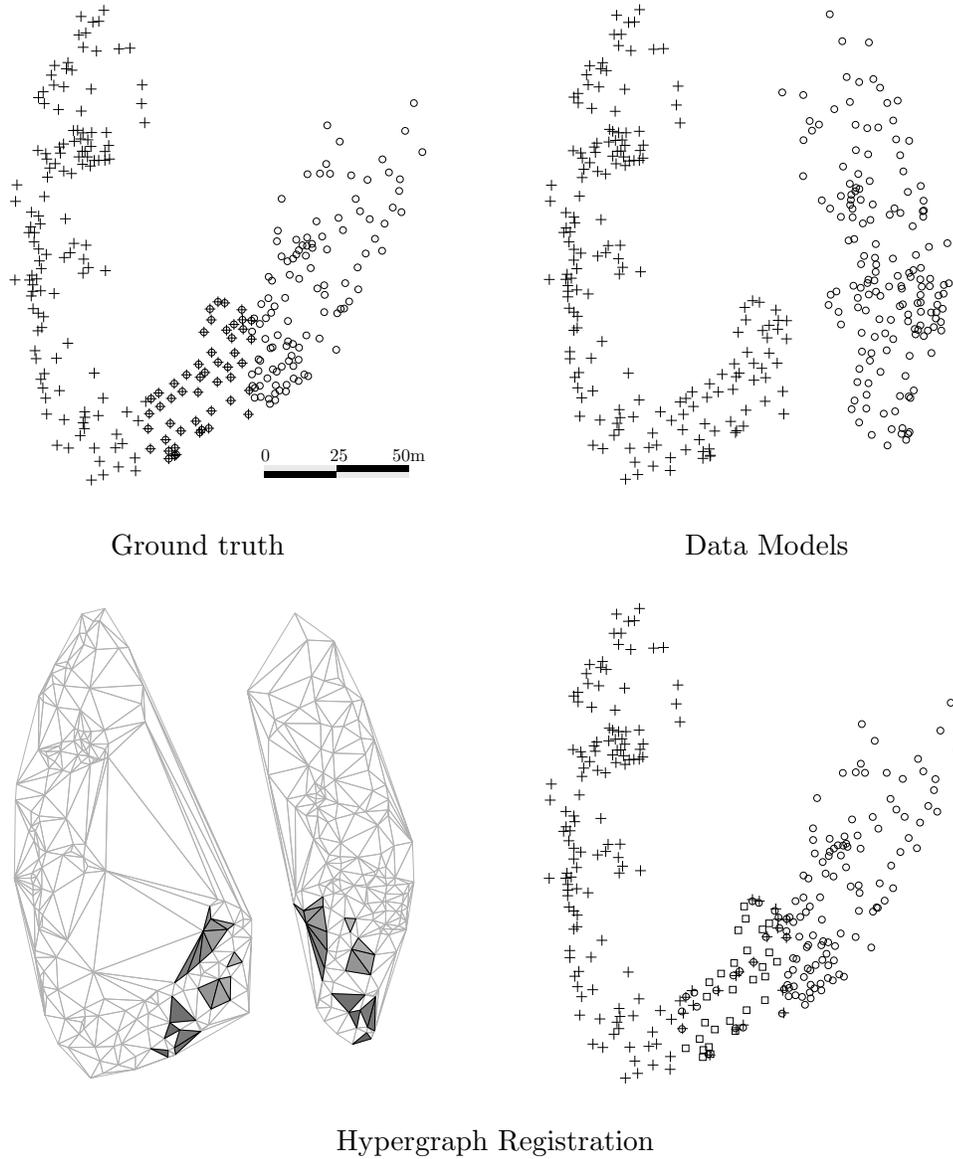
Figure 5.1: Hypergraph registration (Victoria Park example): ground truth and registration solution. (Ground truth) The true landmark locations observed by agent p and agent q are indicated by crosses (+) and circles ($\circ$), respectively. The agents observe 50 landmarks in common (contained by the vector μ) with agent p observing 179 landmarks (contained by u_p) and agent q observing 160 landmarks (contained by u_q). (Data models) The individual stochastic maps of the agents are generated using an additive Gaussian noise model, with the map of agent q being transformed into a separate coordinate system by θ and t. (Hypergraph registration) Using linear programming and outlier rejection, an inlier set of 16 common directed triangles (shaded in gray) are used to estimate the common landmark parameters of the data models.
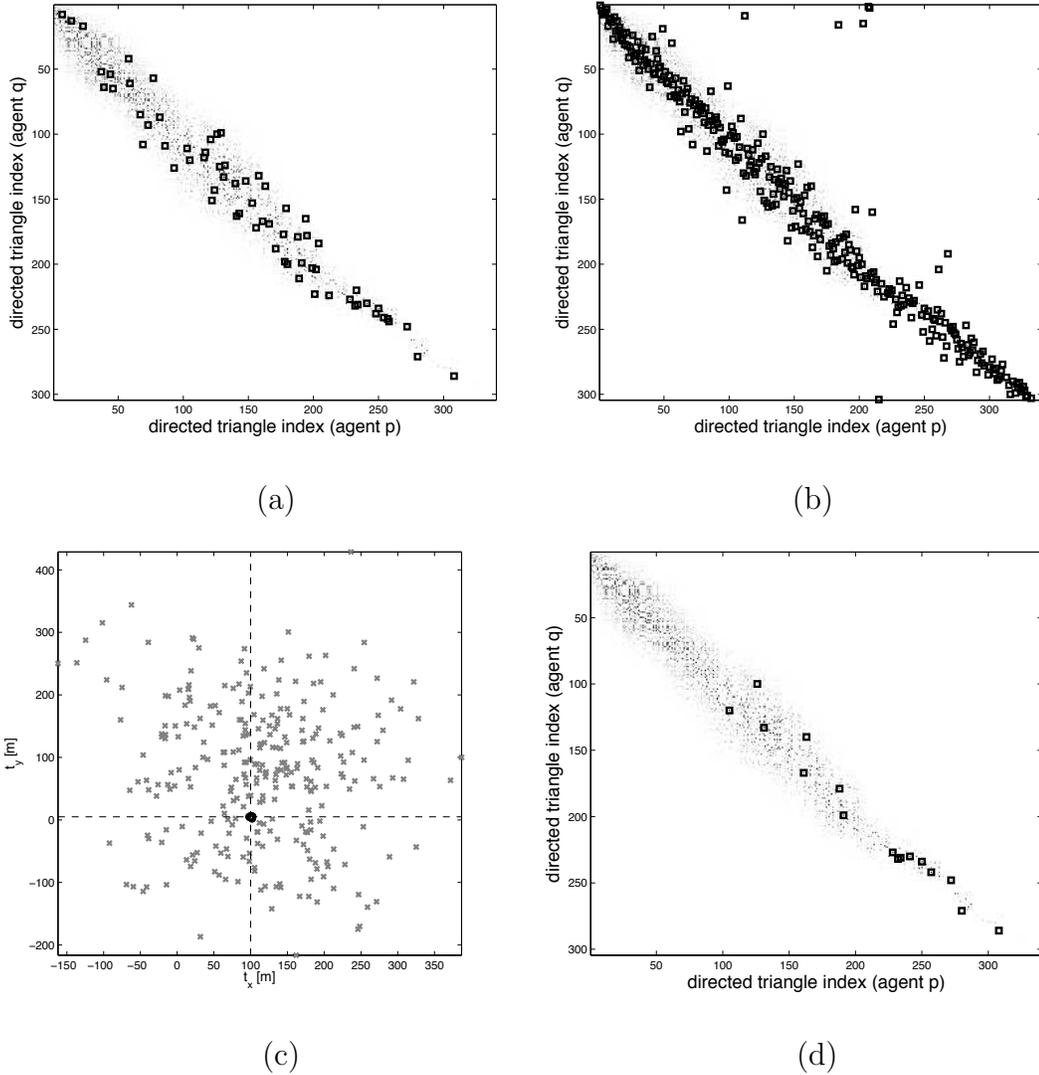
Figure 5.2: Hypergraph registration (Victoria Park example): likelihood statistics and outlier rejection. Markers are used to indicate entries of the likelihood matrix Δ corresponding to (a) the true directed triangle matches, (b) the triangle matches specified by the linear program. (c) Inlier matches (black circles) are indicated by the rigid-body transform parameters that cluster around the true values of t and θ, with outliers (gray crosses) indicated by the entries that fall outside the cluster. (d) After applying outlier rejection to the output of the linear program, 16 inlier matches are used to construct the registration solution $\mathcal{R}^*$.

5.2   Monte Carlo experiments

This section considers the performance of the data fusion rules proposed in Section 2.4 and the hypergraph registration approach described in Section 4.3. Monte Carlo results are provided by considering the performance of the approach when applied to large scale experimental models (Fig. 4.3) and small scale synthetic models (Fig. 4.4) of natural and semi-structured environments over a wide range of noise and landmark overlap, as illustrated in Fig. 5.3.

The Monte Carlo performance of the proposed data registration approach (see Section 4.3) is evaluated over varying levels of landmark overlap and noise using the ground truth hypergraph models shown in Fig. 5.4. The performance is evaluated using both synthetic and experimental ground truth models, which exhibit a similar
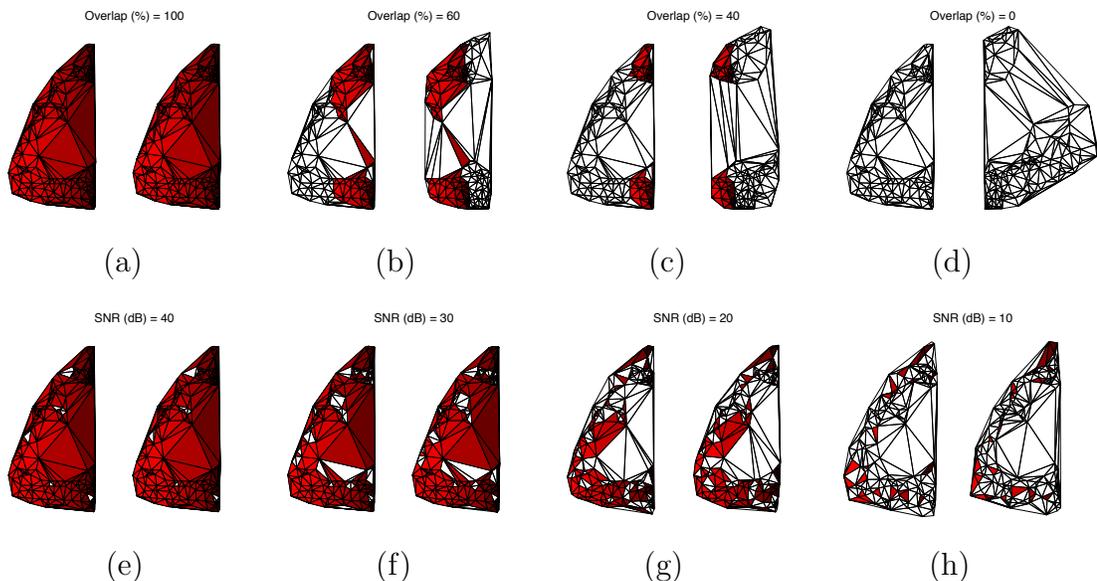
Figure 5.3: Illustration of overlap and noise models. Hypergraph models are shown above for a fusion agent p (left) and a data contributor q (right) in various overlap and noise scenarios. The top row illustrates common triangles (red) and uncommon triangles (white) in hypergraphs of (a) 100%, (b) 60%, (c) 40% and (d) 0% overlap. The bottom row (e-h) illustrates the impact of noise at a fixed overlap of 100%.

structure of the likelihood matrix Δ (bottom row of Fig. 5.4). The edge lengths $\{\ell_i\}$ of each graph are used to compute the signal variance given by $\sigma_s^2 = \frac{1}{m} \sum_{i=1}^{m} \ell_i^2$. A noise variance is computed as $\sigma_n^2 = 2\sigma^2$ since zero-mean Gaussian noise is added to the individual vertices of each edge with a variance of σ^2. Using the signal variance σ_s^2 and noise variance σ_n^2, the signal-to-noise ratio (SNR) in decibels is then $\mathrm{SNR_{dB}} = 10 \log(\sigma_s^2 / \sigma_n^2)$. The noise level of each Monte Carlo experiment is thus specified by solving for the noise variance σ_n^2 as a function of the signal variance and SNR.

(a)   (b)   (c)   (d)
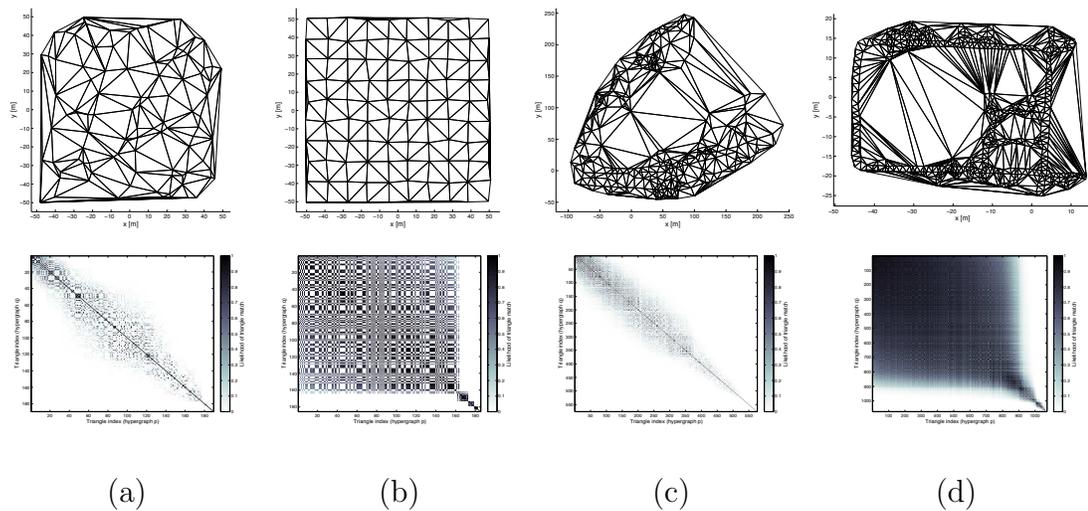
Figure 5.4: Ground truth models and likelihood structure. The top row shows Delaunay triangulations of ground truth points computed from (a) 100 points (189 triangles) drawn from a uniform distribution, (b) 100 points (185 triangles) arranged in a deterministic grid with additive noise, (b) the Victoria Park example with 299 points (576 triangles) and (d) the DLR example with 549 points (1073 triangles). The bottom row shows the likelihood matrix Δ associated with each model. The figure illustrates similarities in Δ between the natural environment models of (a) and (c) and the semi-structured models of (b) and (d).

Four metrics of performance are illustrated in Fig. 5.5:

1. the *true percentage of common triangles* relative to the ground truth model of the environment,

2. the *percentage of true positive triangle assignments* determined by the solution of the linear assignment problem,

3. the *absolute difference* (normalized as a percentage) indicating the difference between the true percentage of common triangles and the percentage true positives and

4. the *percentage of matched (inlier) triangle assignments* (relative to the true number of common triangles) after applying outlier rejection.

The results indicate a graceful degradation in performance with decreasing SNR. However, the approach begins to break down in the noise range of $\text{SNR}_{\text{dB}} \leq$ 20 dB due to either a lack of (or inability to detect) common triangles. The resulting data fusion mean square error (MSE) relative to the coordinate system of fusion agent is shown in Fig. 5.6.
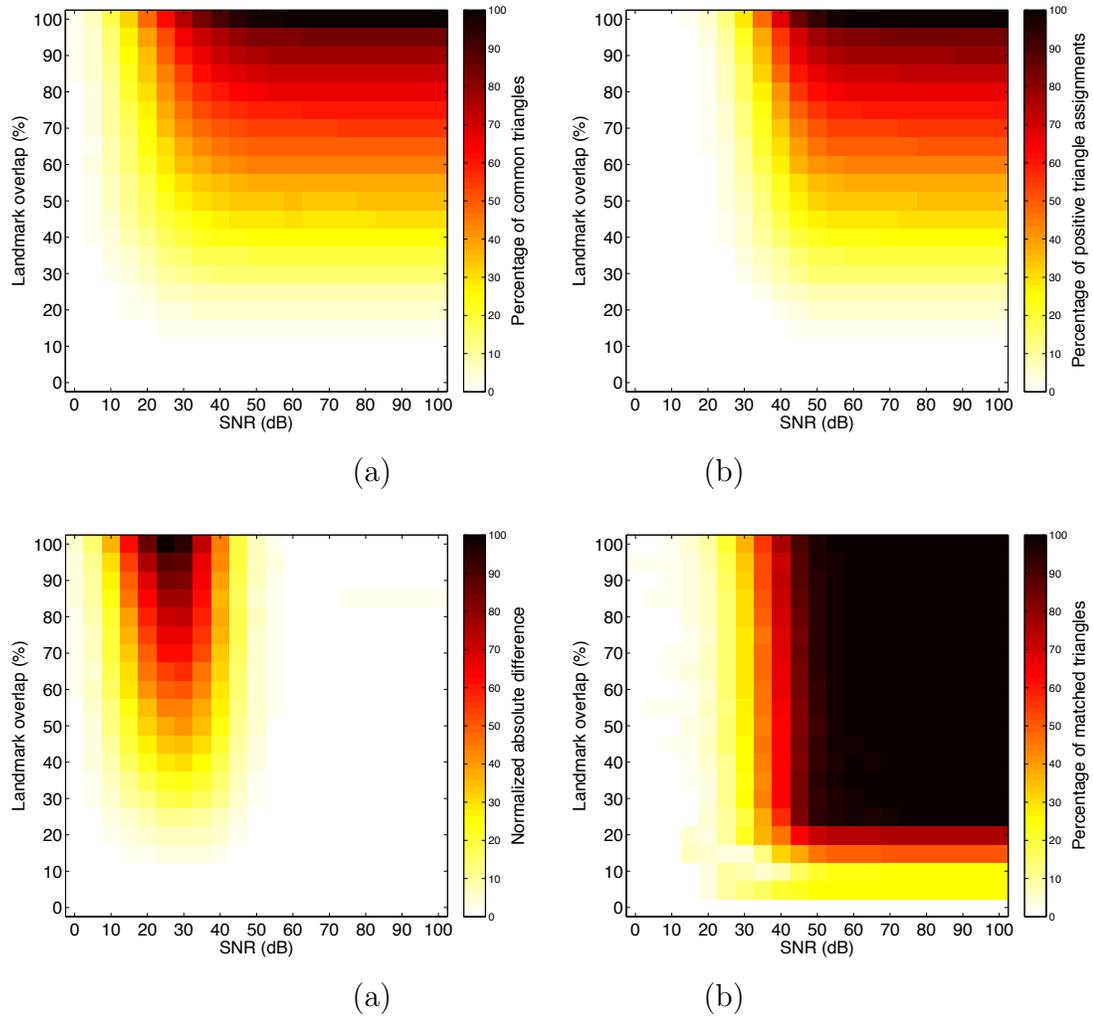
Figure 5.5: Monte Carlo performance of hypergraph matching. Varying the levels of noise and overlap results in a change in (a) the percentage actual common triangles relative to the ground truth of G_p and G_q and (b) the number of true positive common triangles determined by the linear assignment problem (LAP). The absolute difference between (a) and (b), normalized as a percentage, is shown in (c), which shows that the difference between the LAP solution and ground truth is small for a reasonably wide range of overlap and noise, resulting in the percentages of matched triangles after outlier rejection shown in (d).
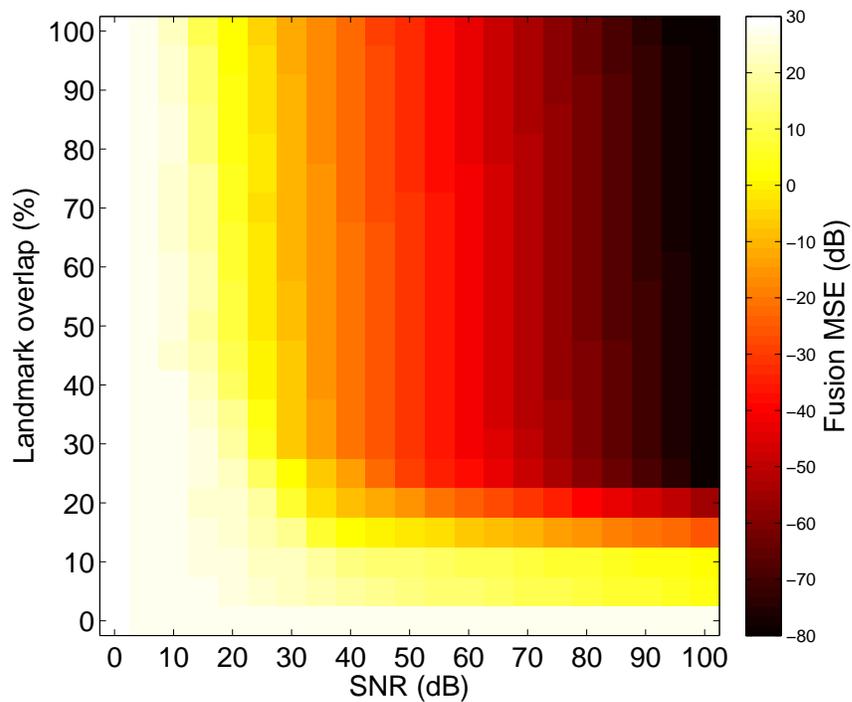
Figure 5.6: Monte Carlo MSE (in dB) performance. The plot shows that in the range of 15%-100% overlap in landmarks, the data fusion MSE exhibits a linear degradation in performance with decreasing SNR. However, the data fusion MSE is relatively high at all noise levels below a 15% overlap in landmarks due to a general lack of common triangles.

CHAPTER 6

CONCLUSION

This thesis considered the problem of constructing a global map of landmarks from the data models contributing agents. The problem can be formulated as a mixed integer-parameter estimation problem from which landmarks common to a fusion agent and data contributor are registered under a global coordinate system. Under this framework, the optimal fusion of stochastic maps can be accomplished using the maximum likelihood principle. Unfortunately, however, the complexity of the true ML solution is prohibitive, which leads to a partitioning of data fusion into two main parts: (i) data registration using a bipartite directed hypergraph matching using generalized likelihood ratio statistics and (ii) parameter estimation to obtain the estimated of the combined map under a common coordinate frame.

The main advantage of the proposed approach is the comprehensive nature of the procedure: a global map is found in spite of the individual data models being obtained in separate coordinate systems without prior knowledge of common landmarks. The performance of the proposed approach is found to be reasonable at high SNR but deteriorates gracefully with increasing noise, which is largely due to a decrease in common directed triangles. One way to improve the performance would be to impose neighborhood and adjacency constraints on the hypergraph model. Further computation gains may also be found by exploiting the banded structure of the likelihood matrix Δ.

With continual advances in sensors and computational ability, the future of mobile robotics is bright. With any hope, the techniques proposed in this thesis will help pave the way to increased autonomy in multi-agent perception and navigation systems, as shown in Fig. 6.1.

Figure 6.1: The author with several robotic agents. In the absence of a global frame of reference, a global metric model of an environment is constructed from the data models of multiple robotic agents (such as those pictured above) by applying data fusion techniques of the nature proposed in this thesis.

APPENDIX

A.1   Review of sigma point filter

This section reviews the *sigma point filter* [40] (illustrated in Fig. A.1) as an example algorithm for constructing metric data models of an environment. Sigma points, denoted by $\mathcal{X}_{k-1}^{[0]}, \mathcal{X}_{k-1}^{[1]}, \ldots, \mathcal{X}_{k-1}^{[2L]}$ where k is a time index, are variables drawn from the multivariate normal distribution using a deterministic sigma point sampler given by

$$
\mathcal{X}_{k-1}^{[i]} = \begin{cases} \hat{x}_{k-1} & \text{for} \quad i = 0 \\ \hat{x}_{k-1} + \sqrt{(L + \lambda)\, \Sigma_{i,k-1}} & \text{for} \quad i = 1, \ldots, L \\ \hat{x}_{k-1} - \sqrt{(L + \lambda)\, \Sigma_{i-L,k-1}} & \text{for} \quad i = L+1, \ldots, 2L \end{cases}
$$

where L is the dimension of the state estimate (i.e., $\hat{x}_{k-1} \in \mathbb{R}^L$) and the parameter $\lambda = \alpha^2(L + \kappa) - L$ determines the spread of the sigma points. The notation $\Sigma_{i,k-1}$ denotes column i of the covariance matrix Σ_{k-1}. Sigma points are also characterized by the weights

$$
w_m^{[0]} = \lambda(L + \lambda)^{-1}
$$

$$
w_c^{[0]} = \lambda(L + \lambda)^{-1} + (1 - \alpha^2 + \beta)
$$

$$
w_m^{[i]} = w_c^{[i]} = [2(L + \lambda)]^{-1} \quad \text{for} \quad i = 1, \ldots, 2L
$$

where $w_m^{[\cdot]}$ and $w_c^{[\cdot]}$ are weights associated with mean and covariance, respectively (choose $\beta = 2$ for Gaussian distributions [40]). Using the notation $\gamma = \sqrt{(L + \lambda)}$ for brevity, the sigma point filter (also known as the *unscented Kalman filter*, or UKF), is specified given a nonlinear process model $f(\cdot)$, with control input u_k at time-step k, and nonlinear measurement model $h(\cdot)$ as follows.
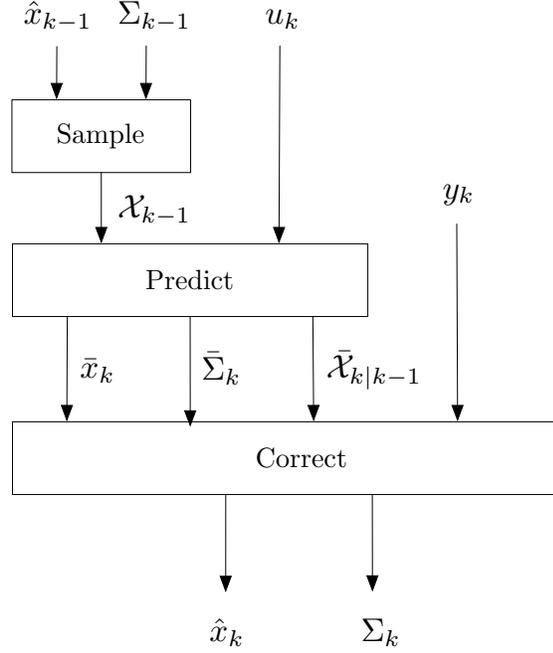
Figure A.1: Block diagram of sigma point filter.

A.1.1 Sample

$$\mathcal{X}_{k-1}^{[i]} = \hat{x}_{k-1} \qquad \text{for} \quad i = 0$$

$$\mathcal{X}_{k-1}^{[i]} = \hat{x}_{k-1} + \gamma\sqrt{\Sigma_{i,k-1}} \qquad \text{for} \quad i = 1,\ldots,L$$

$$\mathcal{X}_{k-1}^{[i]} = \hat{x}_{k-1} - \gamma\sqrt{\Sigma_{i-L,k-1}} \quad \text{for} \quad i = L+1,\ldots,2L$$

A.1.2 Predict

$$\bar{\mathcal{X}}_{k|k-1}^{[i]} = f\left(\mathcal{X}_{k-1}^{[i]}, u_k\right) \quad \text{for} \quad i = 0,\ldots,2L$$

$$\bar{x}_k = \sum_{i=0}^{2L} w_m^{[i]} \bar{\mathcal{X}}_{k|k-1}^{[i]}$$

$$\bar{\Sigma}_k = \sum_{i=0}^{2L} w_c^{[i]} \left(\bar{\mathcal{X}}_{k|k-1}^{[i]} - \bar{x}_k\right)\left(\bar{\mathcal{X}}_{k|k-1}^{[i]} - \bar{x}_k\right)^T + Q_k$$

A.1.3 Correct

Sigma-point update

$$\bar{\mathcal{X}}_{k|k}^{[i]} = \bar{x}_k \qquad\qquad \text{for} \quad i = 0$$

$$\bar{\mathcal{X}}_{k|k}^{[i]} = \bar{x}_k + \gamma\sqrt{\bar{\Sigma}_{i,k}} \qquad \text{for} \quad i = 1, \ldots, L$$

$$\bar{\mathcal{X}}_{k|k}^{[i]} = \bar{x}_k - \gamma\sqrt{\bar{\Sigma}_{i-L,k}} \quad \text{for} \quad i = L+1, \ldots, 2L$$

Measurement prediction

$$\bar{\mathcal{Y}}_{k}^{[i]} = h\left(\bar{\mathcal{X}}_{k|k}^{[i]}\right) \quad \text{for} \quad i = 0, \ldots, 2L$$

$$\bar{y}_k = \sum_{i=0}^{2L} w_m^{[i]} \bar{\mathcal{Y}}_{k}^{[i]}$$

Kalman update (with measurement noise covariance R_k)

$$S_k = \sum_{i=0}^{2L} w_c^{[i]} \left(\bar{\mathcal{Y}}_{k}^{[i]} - \bar{y}_k\right)\left(\bar{\mathcal{Y}}_{k}^{[i]} - \bar{y}_k\right)^T + R_k$$

$$W_k = \left(\sum_{i=0}^{2L} w_c^{[i]} \left(\bar{\mathcal{X}}_{k|k}^{[i]} - \bar{x}_k\right)\left(\bar{\mathcal{Y}}_{k}^{[i]} - \bar{y}_k\right)^T\right) S_k^{-1}$$

$$\hat{x}_k = \bar{x}_k + W_k\left(y_k - \bar{y}_k\right)$$

$$\Sigma_k = \bar{\Sigma}_k - W_k S_k W_k^T.$$

BIBLIOGRAPHY

[1] R. Smith, M. Self, and P. Cheeseman, "A stochastic map for uncertain spatial relationships," in *Proceedings of the Fourth International Symposium on Robotics Research.* Cambridge, MA, USA: MIT Press, 1988, pp. 467–474. [Online]. Available: http://dl.acm.org/citation.cfm?id=57425.57472

[2] ——, "Estimating uncertain spatial relationships in robotics," in *Autonomous Robot Vehicles.* Springer-Verlag New York, Inc., 1990, vol. 8, pp. 167–193.

[3] Y. Zhou, H. Leung, and P. Yip, "An exact maximum likelihood registration algorithm for data fusion," *IEEE Transactions on Signal Processing*, vol. 45, no. 6, pp. 1560–1573, 1997.

[4] R. Viswanathan and P. Varshney, "Distributed detection with multiple sensors I: Fundamentals," *Proceedings of the IEEE*, vol. 85, no. 1, pp. 54–63, 1997.

[5] R. Blum, S. Kassam, and H. Poor, "Distributed detection with multiple sensors II: Advanced topics," *Proceedings of the IEEE*, vol. 85, no. 1, pp. 64–79, 1997.

[6] J. Chamberland and V. Veeravalli, "Decentralized detection in sensor networks," *IEEE Transactions on Signal Processing*, vol. 51, no. 2, pp. 407–416, 2003.

[7] R. Niu, B. Chen, and P. Varshney, "Fusion of decisions transmitted over Rayleigh fading channels in wireless sensor networks," *IEEE Transactions on Signal Processing*, vol. 54, no. 3, pp. 1018–1027, 2006.

[8] M. Dissanayake, P. Newman, S. Clark, H. Durrant-Whyte, and M. Csorba, "A solution to the simultaneous localization and map building (SLAM) problem," *IEEE Transactions on Robotics and Automation*, vol. 17, no. 3, pp. 229–241, Jun 2001.

[9] H. Durrant-Whyte and T. Bailey, "Simultaneous localization and mapping (SLAM): Part I," *IEEE Robotics and Automation Magazine*, vol. 13, no. 2, pp. 99–110, 2006.

[10] ——, "Simultaneous localization and mapping (SLAM): Part II," *IEEE Robotics and Automation Magazine*, vol. 13, no. 3, pp. 108–117, 2006.

[11] S. Thrun and Y. Liu, "Multi-robot SLAM with sparse extended information filers," in *Proceedings of the 11th International Symposium of Robotics Research.* Sienna, Italy: Springer, 2003.

[12] D. Hall and J. Llinas, "An introduction to multisensor data fusion," *Proceedings of the IEEE*, vol. 85, no. 1, pp. 6–23, 1997.

[13] N. Katayama and S. Satoh, "The SR-tree: An index structure for high-dimensional nearest neighbor queries," in *Proceedings of the 1997 ACM SIGMOD International Conference on Management of Data*, ser. SIGMOD '97. New York, NY, USA: ACM, 1997, pp. 369–380.

[14] S. Grime and H. Durrant-Whyte, "Data fusion in decentralized sensor networks," *Control Engineering Practice*, vol. 2, no. 5, pp. 849 – 863, 1994. [Online]. Available: http://www.sciencedirect.com/science/article/pii/0967066194903492

[15] S. Sukkarieh, E. Nettleton, J.-H. Kim, M. Ridley, A. Goktogan, and H. Durrant-Whyte, "The ANSER project: Data fusion across multiple uninhabited air vehicles," *The International Journal of Robotics Research*, vol. 22, no. 7-8, pp. 505–539, July 2003.

[16] S. Julier and J. Uhlmann, "A non-divergent estimation algorithm in the presence of unknown correlations," in *Proceedings of the American Control Conference*, vol. 4, 1997, pp. 2369–2373.

[17] J. Tardós, J. Neira, P. Newman, and J. Leonard, "Robust mapping and localization in indoor environments using sonar data," *International Journal of Robotics Research*, vol. 21, no. 4, pp. 311–330, 2002.

[18] J. Castellanos, R. Martinez-Cantin, J. Tardós, and J. Neira, "Robocentric map joining: Improving the consistency of EKF-SLAM," *Robotics and Autonomous Systems*, vol. 55, no. 1, pp. 21–29, 2007.

[19] S. B. Williams, G. Dissanayake, and H. F. Durrant-Whyte, "Towards multi-vehicle simultaneous localisation and mapping," in *IEEE International Conference on Robotics and Automation (ICRA)*, 2002, pp. 2743–2748.

[20] X. Zhou and S. Roumeliotis, "Multi-robot SLAM with unknown initial correspondence: The robot rendezvous case," in *International Conference on Intelligent Robots and Systems*, oct. 2006, pp. 1785 –1792.

[21] L. Andersson and J. Nygards, "C-SAM: Multi-robot SLAM using square root information smoothing," in *International Conference on Robotics and Automation*, 2008, pp. 2798–2805.

[22] D. Benedettelli, A. Garulli, and A. Giannitrapani, "Multi-robot SLAM using M-Space feature representation," in *IEEE Conference on Decision and Control*, 2010, pp. 3826 –3831.

[23] R. Aragues, J. Cortes, and C. Sagues, "Distributed consensus algorithms for merging feature-based maps with limited communication," *Robotics and Autonomous Systems*, vol. 59, no. 3-4, pp. 163–180, 2011.

[24] E. Groth, "A pattern-matching algorithm for two-dimensional coordinate lists," *The Astronomical Journal*, vol. 91, no. 5, pp. 1244–1248, 1986.

[25] H. Ogawa, "Labeled point pattern matching by Delaunay triangulation and maximal cliques," *Pattern Recognition*, vol. 19, no. 1, pp. 35–40, 1986.

[26] B. Delaunay, "Sur la sphère vide," *Izvestia Akademii Nauk SSSR, Otdelenie Matematicheskikh i Estestvennykh Nauk*, vol. 7, pp. 793–800, 1934.

[27] H. Cramér, "A contribution to the theory of statistical estimation," *Skandinavisk Aktuaries Tidskrif*, vol. 29, pp. 458–463, 1946.

[28] ——, *Mathematical Methods of Statistics*.   Princeton, NJ, USA: Princeton University Press, 1946.

[29] C. R. Rao, "Minimum variance and the estimation of several parameters," in *In Proceedings of Cambridge Philosophical Society*, 1946, pp. 280–283.

[30] ——, *Linear Statistical Inference and Its Applications, Second Edition*.   New York, NY, USA: John Wiley & Sons, Inc., 1973.

[31] S. M. Kay, *Fundamentals of statistical signal processing: Estimation theory*. Upper Saddle River, NJ, USA: Prentice-Hall, Inc., 1993.

[32] W. W. Hager, "Updating the inverse of a matrix," *SIAM Review*, vol. 31, no. 2, pp. 221–239, 1989.

[33] H. W. Kuhn, "The Hungarian method for the assignment problem," *Naval Research Logistics Quarterly*, vol. 2, no. 1-2, pp. 83–97, 1955.

[34] D. Luenberger and Y. Ye, *Linear and Nonlinear Programming, 3rd edition.* New York, NY: Springer, 2008.

[35] R. Jonker and A. Volgenant, "A shortest augmenting path algorithm for dense and sparse linear assignment problems," *Computing*, vol. 38, no. 4, pp. 325–340, 1987.

[36] O. Faugeras and M. Hebert, "The representation, recognition, and locating of 3-D objects," *International Journal of Robotics Research*, vol. 5, no. 3, pp. 27–52, 1986.

[37] J. B. Kuipers, "Quaternions and rotation sequences," in *Proceedings of the First International Conference on Geometry, Integrability and Quantization*, 2000, pp. 127–143.

[38] M. A. Fischler and R. C. Bolles, "Random sample consensus: A paradigm for model fitting with applications to image analysis and automated cartography," *Communications of the ACM*, vol. 24, no. 6, pp. 381–395, 1981.

[39] S. Huang, Z. Wang, and G. Dissanayake, "Sparse local submap joining filter for building large-scale maps," *IEEE Transactions on Robotics*, vol. 24, no. 5, pp. 1121–1130, 2008.

[40] R. van der Merwe and E. Wan, "Sigma-point Kalman filters for probabilistic inference in dynamic state-space models," in *In Proceedings of the Workshop on Advances in Machine Learning*, 2003.